Advances in Water Resources 109 (2017) 106–120

Contents lists available at ScienceDirect

Advances in Water Resources

journal homepage: www.elsevier.com/locate/advwatres

Four decades of microwave satellite soil moisture observations: Part 1. A review of retrieval algorithms

L. Karthikeyan[a,b,*], Ming Pan[a], Niko Wanders[a,c], D. Nagesh Kumar[b], Eric F. Wood[a]

[a] Department of Civil and Environmental Engineering, Princeton University, NJ, USA
[b] Department of Civil Engineering, Indian Institute of Science, Bangalore, India
[c] Department of Physical Geography, Utrecht University, Utrecht, The Netherlands

ARTICLE INFO

Article history:
Received 27 February 2017
Revised 2 September 2017
Accepted 5 September 2017
Available online 6 September 2017

Keywords:
Soil moisture
Retrieval algorithm
Passive microwave
Active microwave
Radiative transfer model
Change detection model

ABSTRACT

The satellite based passive (radiometer) and active (radar) microwave sensors enhanced our ability to retrieve soil moisture at global scales. It has been almost four decades since the first passive microwave satellite sensor was launched in 1978. Since then soil moisture has gained considerable attention in hydro-meteorological, climate, and agricultural research resulting in the deployment of two dedicated missions in the last decade, SMOS and SMAP. Microwave retrievals require an algorithm to estimate soil moisture from satellite measurements. In this Part 1 of a two-part review series, we provide a synthesis of four decades of research and development on the passive and active microwave soil moisture retrieval algorithms. The algorithms associated with passive sensors use the radiometer brightness temperatures, while active sensors use the radar backscatter measurements to retrieve soil moisture. The physics of both algorithm classes are based on the fact that the microwave measurements at lower frequencies are influenced by the soil dielectric property, which acts as a proxy for the surface soil moisture content. In this review effort, the emphasis is laid on the physical models of the passive and the active retrieval algorithms. These algorithms facilitate to obtain the individual radiative contributions from soil, vegetation, and atmosphere that reach satellite sensors after mixing (roughness), scattering, and attenuation. In the process, we looked into the current research efforts to improve individual aspects of the algorithms, followed by a description of different retrieval procedures. In Part 2 of this review series, performance evaluation and inter-sensor comparisons of soil moisture of eight passive and two active sensors are carried out using 1058 stations along with model soil moisture data in the Contiguous United States (CONUS) region.

1. Introduction

Soil moisture is an important variable that plays a vital role in linking the global terrestrial water, energy and carbon cycles. It quantitatively describes the amount of water present in the pore spaces of unsaturated soil expressed in terms of volumetric units (m^3_{water}/m^3_{soil}), depth units (mm_{water}/mm_{soil}), mass units (kg_{water}/m^2_{soil}), or in the form of relative soil moisture ($SM_{actual}/SM_{saturation}$), depending on the manner in which it is measured. Soil moisture has a significant effect on water and energy exchanges at the land-atmosphere interface. It impacts climate processes such as precipitation (Berg et al., 2017; Koster et al., 2004), temperature (Berg et al., 2014), and evapotranspiration (Seneviratne et al., 2010), and is responsible for the partitioning of precipitation into runoff and storage (Wagner et al., 2003). Over the past four decades, microwave remote sensing has evolved into an important tool that facilitates the measurement of soil moisture at global scales. It created an opportunity to involve soil moisture in several hydro-meteorological, climate and agricultural applications such as drought monitoring (Bolten et al., 2010), flood forecasting (Wanders et al., 2014b; Alvarez-Garreton et al., 2015), precipitation estimates (Wanders et al., 2015; Zhan et al., 2015), crop yield (Manzoni et al., 2013), weather forecasting (Drusch et al., 2009) and the calibration of hydrological model parameters (Wanders et al., 2014a).

Some advantages of microwave remote sensing over other remote sensing techniques include: (a) the dielectric properties of the soil-water medium are highly sensitive to the water content in soil due to significant differences between the dielectric constants of water and soil. These changes in the dielectric properties are detected through either space-borne surface emissions or backscatter measurements; (b) the negligible influence of the atmosphere; and

* Corresponding author at: Department of Civil Engineering, Indian Institute of Science, Bangalore, India.
E-mail address: karthik120120@gmail.com (L. Karthikeyan).

http://dx.doi.org/10.1016/j.advwatres.2017.09.006
0309-1708/

(c) satellite measurements being independent of solar illumination (Jackson 1993). In general, the soil moisture retrievals are carried out using microwave data at low frequencies (as the vegetation attenuation has a lower impact for higher frequencies (Calvet et al., 2011)). An increase in frequency leads to a reduction in emission originating depth (in soil) along with an increased effect of atmospheric attenuation (Wigneron et al., 2003). The microwave sensors are categorized into passive and active sensors. The passive sensor, i.e. radiometer, measures the naturally emitted energy from the earth surface in the form of brightness temperature (T_B). The active sensor, i.e. radar, sends a focused beam of microwave radiation towards the ground and captures the backscattered signal (σ_o) from the Earth's surface.

The concept of satellite retrieval of soil moisture arises from the fact that the dielectric properties of soil – which act as a proxy for soil moisture – affect the emissivity and backscattering properties of soil surfaces in microwave frequencies. Thus, passive (radiometer) and active (radar) sensors measure brightness temperature, and backscatter to detect the soil moisture variations. In general, L- (0.5–1.5 GHz), C-(4–8 GHz), and X- (8–12 GHz) bands are considered to be soil moisture-sensitive frequency bands (with less emphasis beyond the X-band). In short, moist soil appears cooler for radiometers and brighter for radar. Although microwave observations are less affected by the atmosphere and vegetation cover – which emits and backscatters microwave signals – they still play a significant role in attenuating the soil moisture signals at higher frequencies, making it difficult/impossible to retrieve soil moisture from densely vegetated regions. Moreover, heavy precipitation contributes to noise, making retrievals during active precipitation conditions less reliable. Another form of interference comes from man-made microwave sources, the so-called Radio Frequency Interference (RFI) (Kerr et al., 2012), which leads to an oversaturation of the microwave signal. Most importantly, microwave measurements are sensitive to the top few centimeters of soil layer, usually one tenth to one half of the signal wavelength (Wilheit 1978) resulting in longer wavelength signals having deeper emission (penetration) depth (1–5 cm). Despite retrievals being sensitive to only top soil, the information provided by them can be used to assess the root zone soil moisture (Baldwin et al., 2017; Dumedah et al., 2015) or the column total water (Wagner et al., 1999a), which is a critical variable for weather forecasting (Koster and Suarez 2003), drought analysis (Bolten et al., 2010; Yuan et al., 2015), and carbon cycling modeling (Das et al., 2008).

Nevertheless, attention to the study of soil moisture has been on the rise over the past few decades that needs retrievals with global coverage and improved accuracy. Eight passive microwave satellite missions have been widely utilized for soil moisture estimation, the Scanning Multichannel Microwave Radiometer (SMMR) onboard Nimbus-7 (1978–1987), the Special Sensor Microwave - Imager (SSM/I) onboard Defense Meteorological Satellite Program (DMSP) (1987–2007), the microwave imager onboard Tropical Rainfall Measuring Mission (TRMM) (1997–2015), the WindSAT mission onboard Coriolis (2003–2012), the Advanced Microwave Scanning Radiometer – Earth Observing System (AMSR-E) onboard Aqua satellite (2002–2011), the Advanced Microwave Scanning Radiometer 2 (AMSR2) onboard the GCOM-W satellite (2012-present), along with two dedicated satellite missions, the Soil Moisture Ocean Salinity (SMOS) mission (Kerr et al., 2016), and the Soil Moisture Active Passive (SMAP) mission (Chan et al., 2016). Two active microwave satellite missions have been important for soil moisture estimation: the Scatterometers (SCAT) onboard European Remote Sensing (ERS-1/2) satellites (1991–2011), and the Advanced Scatterometer (ASCAT) onboard the Meteorological Operational satellite program (MetOp-A/B) (2007–2014).

Once the satellite observations are obtained, the retrieval process through which they are converted into soil moisture values will be significantly impacted by the accuracy and skill of the estimates (Mladenova et al., 2014). Hence, it is important to study the intricacies of algorithms used for the soil moisture retrievals from these sensors. In this Part 1 of the two-part review series, we look at the development of passive and active microwave retrieval algorithms intended for soil moisture retrievals over the last four decades. Section 2 presents a review of passive microwave retrieval algorithms. Section 3 provides a review of active microwave retrieval algorithms. Some of the key aspects of the retrieval algorithms are later on discussed in Section 4. Part 2 of this review series deals with the evolution of passive and active microwave instruments, and the validation of soil moisture from the aforementioned eight passive and two active microwave sensors using station (International Soil Moisture Network – ISMN) observations and model (Variable Infiltration Capacity – VIC) simulations over the Contiguous United States (CONUS) region.

2. Retrieval of soil moisture from passive microwave sensors

In 1970s, it was recognized that passive microwave sensor measurements are useful for estimating surface soil moisture content (Burke and Paris 1975; Eagleman and Lin 1976; Newton 1977; Njoku and Kong 1977; Poe and Edgerton 1971; Poe et al., 1971; Schmugge 1978; Schmugge et al., 1974; Schmugge et al., 1980). The microwave radiometers detect the thermal emission (in the form of brightness temperature T_B) from soil surface which is proportional to the soil physical temperature (T_S). The constant of proportionality is the soil microwave emissivity (ε) (Eq. (1)), which is influenced strongly by soil moisture variations (Schmugge 1987). Emissivity, according to the Kirchhoff's law (Kirchhoff 1860), complements the surface reflectivity (R), $\varepsilon = 1 - R$. As the moisture content in soil increases, the soil dielectric conductivity decreases resulting in a reduction of the emissivity leading to a lower brightness temperature.

$$T_B = \varepsilon \cdot T_S = (1 - R) \cdot T_S \tag{1}$$

The energy emitted from the Earth's surface is proportional to the frequency of the microwave radiation (Planck Einstein relation) and of the natural emissions is very weak at soil moisture sensitive frequencies. This results in coarse resolution of brightness temperature measurements as the microwave radiometers need to look at a larger area in order to detect weak emissions. Moreover, it is now widely accepted to use the L-band frequency for soil moisture retrievals, which further reduces the spatial resolution, despite the need for a large antenna/aperture size, which increases the cost of the sensor. However, the spatial resolution can be improved by using larger antenna pattern and lower orbital altitude. A retrieval algorithm of soil moisture typically has two phases, first, using a Radiative Transfer Model (RTM) to relate T_B and soil dielectric constant (κ) and second, linking soil dielectric constant with soil moisture using 'dielectric mixing' models. Since 1970s, there have been efforts towards improving and evaluating the RTMs for smooth as well as rough soils (Njoku and Kong 1977; Stogryn 1970; Wilheit 1978). The general scheme of radiative transfer equation was formalized by Ulaby et al. (1982). This development was assisted by several experiments involving airborne sensors (Blinn and Quade 1972; Poe and Edgerton 1971; Schanda et al., 1978), satellites (Eagleman and Lin 1976; Hofer and Njoku 1981; Schmugge et al., 1977), and field campaigns (Burke et al., 1979; Choudhury et al., 1979; Schmugge et al., 1974) which helped researchers to ascertain in detail the relationship between emissivity of microwave signals and soil moisture under varied sensor features (i.e., frequency, polarization, and incidence angle), surface characteristics (i.e., surface roughness, soil texture, vegetation and temperature) and atmospheric effects. These assessments lead to modeling the contribution of five important factors: temperature,

Table 1
Summary of dielectric mixing models.

No.	Model	Inputs (units)	Reference
1	Wang and Schmugge model	• Soil moisture (m^3/m^3) • Clay (%) • Sand (%) • Porosity (-)	Wang and Schmugge (1980)
2	Topp Model	• Soil moisture (m^3/m^3)	Topp et al. (1980)
3	Dobson Model	• Microwave frequency (Hz) • Soil moisture (m^3/m^3) • Soil temperature (°C) • Clay (%) • Sand (%) • Dry soil bulk density (g/cm^3) • Solid particle density (g/cm^3) • Soil water salinity (ppt)	Dobson et al. (1985)
4	Hallikanen Model	•Soil moisture (m^3/m^3) • Clay (%) • Sand (%)	Hallikainen et al. (1985)
5	Roth Model	• Soil moisture (m^3/m^3) • Porosity (-) • Dielectric of solid, aqueous and gaseous phases	Roth et al. (1990)
6	Mironov Model	• Soil temperature (°C) • Soil moisture (m^3/m^3) • Clay (%)	Mironov et al. (2009)

surface roughness, vegetation, atmosphere and cosmic background while measuring the T_B (Choudhury et al., 1979; Drusch et al., 2001; Hofer and Njoku 1981; Jackson and Schmugge 1991; Kerr and Njoku 1990; Kirdiashev et al., 1979; Mo and Schmugge 1987; Ulaby et al., 1983; Wang and Choudhury 1981) which were applied to the $\tau - \omega$ vegetation model proposed by Mo et al. (1982) that acts as a baseline for most of the RTMs. The $\tau - \omega$ model is a zeroth order radiative transfer model, which neglects multiple scattering effects (Tsang et al., 1985; Ulaby et al., 1986). This model has two parameters, the vegetation optical depth (VOD) – τ_C, and the single scattering albedo – ω.

In addition, efforts were focused on linking soil moisture with soil dielectric constant using semi-empirical mechanisms and field observations. The dielectric constant of soil is a complex number ($\kappa = \kappa' + i\kappa''$) with the real part ($\kappa'$) describing the propagation of the signal through the soil and the imaginary part (κ'') characterizing the energy loss in the soil. At low frequencies (L-, C-, X- bands), the effect of κ'' is negligible (Dobson et al., 1985; Hallikainen et al., 1985; Wang and Schmugge 1980). Apart from soil moisture, it is also affected by factors such as soil texture, bulk density, instrument frequency, organic content etc. With these aspects under consideration, several dielectric mixing models have been proposed in the literature. Each of the models has been developed using underlying physics and are partly based on several field scale datasets that deal with specific properties of the soil. Important dielectric models and their characteristics are presented in Table 1.

Consider a homogenous soil with a smooth surface. The emissivity of such a soil layer (ε_S) can be estimated from the real part of the soil dielectric constant (κ') using Fresnel's reflectivity equations (Landau and Lifshitz 1960) (Eq. (2)).

$$R_s^H = \left| \frac{\cos\theta - \left(\kappa' - \sin^2\theta\right)^{0.5}}{\cos\theta + \left(\kappa' - \sin^2\theta\right)^{0.5}} \right|^2$$
$$R_s^V = \left| \frac{\kappa'\cos\theta - \left(\kappa' - \sin^2\theta\right)^{0.5}}{\kappa'\cos\theta + \left(\kappa' - \sin^2\theta\right)^{0.5}} \right|^2 \qquad (2)$$

where, θ is the surface incidence angle (relative to normal). Eq. (2) can be substituted in Eq. (1) to obtain polarization dependent, brightness temperature of a smooth soil surface. Eq. (1) also requires surface temperature to compute T_B, which is generally estimated from thermal infrared, high frequency (37 GHz V-polarization) microwave brightness temperatures, or modeled data (Wigneron et al., 2003). In reality, the soil surface is rough by nature which enhances the soil emissions. Hence, the emissivity values estimated from Eq. (2) have to be adjusted accordingly. The soil roughness was theoretically characterized using statistical parameters such as height standard deviation and horizontal correlation length (Tsang et al., 1985), although they are difficult to be implemented in reality (Njoku and Li 1999). A simplified model based on two parameters, h and Q, was proposed by Wang and Choudhury (1981) to calculate reflectivity of rough soils (R_r) which is widely used in retrieval algorithms (Eq. (3)). Here, h parameter characterizes height, and Q is the polarization mixing ratio.

$$R_r^H = \left[(1-Q)\cdot R_s^H + Q\cdot R_s^V\right]\exp\left(-h\cos^2\theta\right)$$
$$R_r^V = \left[(1-Q)\cdot R_s^V + Q\cdot R_s^H\right]\exp\left(-h\cos^2\theta\right) \qquad (3)$$

Several studies in the past have demonstrated the importance of considering roughness effects for accurate retrieval of soil moisture, including the development of alternative roughness models (Wegmüller and Matzler 1999). The roughness effects are directly related to brightness temperature, which in turn reduces the sensitivity to soil moisture (Montpetit et al., 2015). Hence, the impact of these equations was extensively explored in the literature. Field and aircraft campaigns were carried out to estimate the values that parameters h and Q can take under different biomes (Escorihuela et al., 2007; Grant et al., 2008; Jackson and Schiebe 1993; Jackson et al., 1984; Lawrence et al., 2013; McNairn et al., 2015; Mo et al., 1982; Panciera et al., 2014b; Panciera et al., 2009; Peischl et al., 2012; Saleh et al., 2007; Saleh et al., 2004; Wang et al., 1982; Wigneron et al., 2007; Wigneron et al., 2001). In the past, values of h and Q were assumed to be spatially constant (Njoku and Li 1999; Paloscia et al., 2015). This was found to be impacting the retrieval accuracy. Hence, efforts are being focused towards fine tuning the roughness model (Colliander et al., 2016) calibration of roughness models (Fernandez-Moran et al., 2017) or ascertaining the uncertainties caused by roughness parameterizations (Peng et al., 2017) or developing spatially varying surface roughness maps (Wang et al., 2015b) in an attempt to reduce the error in soil moisture retrievals.

On the other hand, it was proposed that the effect of roughness can be merged with the vegetation emission contribution which results in a reduction of the number of unknown parameters in the retrieval algorithm. Such methods have been implemented with measurements from the AMSR-E (Njoku and Chan 2006; Pan et al., 2014), TMI-TRMM (Bindlish et al., 2003) and SMOS (Parrens et al., 2017) sensors. The roughness effects were further investigated by considering the impact of additional parameters that consider the polarization dependent exponent of the cosine term (Wigneron et al., 2007; Wigneron et al., 2001) and polarization dependent roughness parameters (Shi et al., 2002) in Eq. (3). Recently, Fernandez-Moran et al., (2015) carried out a sensitivity analysis of the roughness parameterization using the data from L-band ELBARA-II radiometer. Despite such attention, there is no consensus in this aspect, and it still remains a challenge to quantify roughness at global scales (Karthikeyan et al., 2017).

The above procedure can be implemented for measuring the emissivity under bare soil conditions. In the case when the soil layer is covered with a vegetation canopy, it attenuates soil emissions and hence its effect should be quantified. As mentioned earlier τ_C represents the vegetation optical depth (VOD) and ω the single scattering albedo. τ_C quantifies the leaf and woody components of above ground biomass (Liu et al., 2011). Literature indicates that τ_C can be directly related to the Vegetation Water Content (VWC) (measured as kg/m^2) using the following relationship (Jackson and Schmugge 1991).

$$\tau_C = b \cdot \mathrm{VWC} \tag{4}$$

where, b is a proportionality constant which varies according to vegetation type, microwave frequency and possibly polarization and incidence angle (Jackson and Schmugge 1991). To that effect, Wigneron et al. (2007) have explored the polarization dependency of τ_C and Wigneron et al. (1995) assessed the effect of vegetation structure on τ_C. VWC, on the other hand, can be estimated from visible-near infrared reflectance data through a vegetation index (e.g. the Normalized Difference Vegetation Index (NDVI) (Entekhabi et al., 2014; Grant et al., 2016; Jackson et al., 2004), Leaf Area Index (LAI) (Pellarin et al., 2003a; Saleh et al., 2006a), Enhanced Vegetation Index (EVI) (Justice et al., 1989) or Normalized Difference Water Index (NDWI) (Chen et al., 2005)). However, few algorithms have included the effects of litter and rainfall interception along with that of VWC for the detailed modeling of τ_C (Wigneron et al., 2007). Similarly, few studies have attempted to combine the effects of vegetation and roughness (Bindlish et al. 2003; Njoku and Chan 2006; Pan et al., 2014; Parrens et al., 2017).

The single scattering albedo is defined as a ratio between scattering efficiency to the extinction efficiency within vegetation layer. Its value is dependent on the vegetation type and the leaf characteristics (Van de Griend and Wigneron 2004). Although, it is generally assumed that the scattering effects are minimal in the case of low frequency microwave emissions, resulting in low values being assigned to ω (which are independent of polarization and incidence angle), a sensitivity analysis of the $\tau-\omega$ model carried out by Davenport et al. (2005) revealed the criticality of ω in estimating the soil moisture from vegetated regions. Attempts are now being made into assessing the effects of multiple scattering from the canopy structure on vegetation emissions (Kurum 2013), in developing a spatially varying global single scattering albedo map (Entekhabi et al., 2014; Konings et al., 2016, 2017), in calibrating the single scattering albedo (Fernandez-Moran et al., 2017), and in assessing the implications of considering a temporally varying single scattering albedo on the quality of soil moisture retrievals (Du et al., 2016).

The canopy brightness temperature (T_B^C), measured by ground-based sensors, can be summarized as the summation of three terms (1) soil emission attenuated by vegetation, (2) vegetation emission and (3) ground reflected vegetation emission, hence.

$$T_B^C = T_S \varepsilon_r \Gamma_C + T_C(1-\omega)(1-\Gamma_C) + T_C(1-\omega)(1-\Gamma_C)(1-\varepsilon_r)\Gamma_C \tag{5}$$

where, $\Gamma_C = \exp(-\tau_C \sec\theta)$ is the transmissivity of vegetation structure which is dependent on VOD and incidence angle, while T_S and T_C are the physical temperatures of the soil and the canopy respectively. The surface temperature is dependent on soil properties and moisture content. Hence, some algorithms compute soil temperature as a function of soil type, soil temperature at surface and at a depth, soil moisture or soil dielectric constant, and frequency of radiation (these inputs are obtained from ancillary data sources) (Choudhury et al., 1982; Holmes et al., 2006; Raju et al., 1995; Wigneron et al., 2008; Wigneron et al., 2001). In general, T_S and T_C are assumed to be approximately equal ($T_S \approx T_C$) (Jackson 1993) although few methods compute a composite temperature instead by combining T_S and T_C values obtained from independent sources for soil moisture retrievals (Wigneron et al., 2007). While most retrieval algorithms employ Mo et al. (1982)'s $\tau-\omega$ model to quantify vegetation effects, modifications to this model have been proposed to quantify effectively the scattering effects in moderate to densely vegetated regions (Kurum et al., 2011).

The emissions from bare soil and vegetated surface can also be attenuated by the atmosphere. Considering a land surface that is covered with vegetation, the brightness temperature measured at the top of the atmosphere (T_B^{TOA}) by a sensor is the sum of (1) vegetation and soil emission attenuated by the atmosphere; (2) ground reflected atmospheric emission attenuated twice by the canopy and once by the atmosphere; (3) ground reflected cosmic background (sun) emission attenuated twice by the canopy and atmosphere; and (4) upward atmospheric emission:

$$T_B^{TOA} = T_B^C \Gamma_a + T_B^{a\downarrow}(1-\varepsilon_r)\Gamma_C^2\Gamma_a + T_B^c(1-\varepsilon_r)\Gamma_C^2\Gamma_a^2 + T_B^{a\uparrow} \tag{6}$$

where, $\Gamma_a = \exp(-\tau_a \sec\theta)$ is the transmissivity of the atmosphere with $\tau_a$as the atmospheric optical depth; $T_B^{a\downarrow}$, $T_B^{a\uparrow}$ and T_B^c are the downward atmospheric, upward atmospheric and cosmic background brightness temperatures respectively. The atmospheric optical depth is primarily influenced by oxygen, water vapor and clouds (Kerr and Njoku, 1990), and the atmospheric brightness temperatures depend on the vertical profiles of temperature, gaseous constituents, and liquid droplets in the atmosphere (Kerr et al., 2012). Several studies have accounted for the atmospheric attenuation in microwave frequencies (Choudhury 1993; Drusch et al., 2001; Kerr and Njoku 1990; Kerr et al., 2012; Pellarin et al., 2003b; Prigent et al., 1997). However, if the atmosphere is considered to be transparent (with no attenuations) at low microwave frequencies (Jackson 1993), Eq. (6) is simplified as $T_B^{TOA} = T_B^C$.

It has to be noted that the brightness temperature modeled in the above equations is limited to land surfaces. If a pixel consists of land along with other entities such as water bodies (in the form of lakes, rivers, wetlands, or transient flooding), ice, snow, urban areas, dry sand, and rocks etc., the brightness temperature recorded by the satellite will have a combined response from these entities. Hence, one has to factor out these effects to obtain the brightness temperature emitted from land surface covered with bare or vegetated soils (Entekhabi et al., 2014; Jones et al., 2011; Kerr et al., 2012; Pan et al., 2014).

The algorithm structure involved in soil moisture retrievals (using RTM procedure described above) is governed in two ways, by forward modeling, and by inverse modeling. In forward modeling, the retrieval process begins with a soil moisture value, which acts as an input to dielectric mixing model- Radiative Transfer Equation (RTE) to estimate the corresponding brightness temperature. Based on the error between the observed brightness temperature and its estimated value, the assumed soil moisture value is corrected iteratively. The objective of this optimization procedure is to minimize the error between satellite observed and RTM modeled brightness temperatures. In inverse modeling, the measured brightness temperature corresponding to the polarization that is most sensitive to soil moisture dynamics is selected which is then used in the inverted equations of the RTE and dielectric mixing model to retrieve soil moisture.

The first generation retrieval algorithms were developed based on mono-configuration sensors i.e., single polarization/frequency channel and view angle (Wang et al., 1990). These algorithms retrieve only soil moisture with an objective of minimizing the error between observed and modeled brightness temperatures in the horizontal or the vertical polarization. Parameters such as surface temperature, VOD, and roughness are either obtained from ancillary data/empirical sources or assumed to be constant. Some of the algorithms proposed in this regard are the Single Channel Algorithm (SCA) (Jackson and Schmugge 1989) and the Land Surface Microwave Emission Model (LSMEM) (Drusch et al., 2001; Gao et al., 2004). With the advancements in sensor configurations such as the ones being used in the SMOS and SMAP missions, there arose scope for observing multi angular dual polarization brightness temperatures. In such measurements, the objective function used in the retrieval algorithm can accommodate these factors thereby increasing the number of known observations to estimate the unknown value of soil moisture. The L-band Microwave Emission of the Biosphere Model (L-MEB) (Wigneron et al., 2007) is one such algorithm that is currently in use for the SMOS mission. On the other hand, the Single Channel Algorithm (SCA) is the baseline retrieval algorithm for the SMAP mission.

Since all the passive microwave satellite sensors (SMMR, SSM/I, TMI, WindSAT, AMSR-E, AMSR2, SMOS, and SMAP) have capability of measuring multi frequency/angular dual polarization brightness temperatures, it was thought that the “extra” observations can be used to retrieve simultaneously some additional parameters along with soil moisture. Such an approach reduces the dependency on ancillary data sets thereby removing possible uncertainties in the soil moisture retrievals. This idea resulted in retrieval of multiple parameters. Since VOD is the most important variable that needs to be computed in the retrieval process (whose value was previously obtained from ancillary sources), certain algorithms such as the Dual Channel Algorithm (DCA) (Owe et al., 2001), the 2-Parameter L-band Microwave Emission of the Biosphere (L-MEB) model (Wigneron et al., 2000), the Land Parameter Retrieval Algorithm (LPRM) (Owe et al., 2008), and the revised Land Surface Microwave Emission Model (LSMEM) (Pan et al., 2014), made the retrieval of VOD possible by the aforementioned procedure. These algorithms obtain surface temperature data from ancillary sources of thermal infrared or high frequency microwave brightness temperature measurements. Attempts have been made to reduce such a dependency by simultaneously retrieving surface temperature along with soil moisture and VOD ((Njoku and Li, 1999); 3-Parameter L-MEB model (Wigneron et al., 2000)). Furthermore, the effects of retrieving parameters such as surface roughness (Parrens et al., 2016; Wigneron et al., 2007) and single scattering albedo (Konings et al., 2016), along with soil moisture and VOD have also been successfully explored.

Apart from the physical models, soil moisture is derived from passive microwave measurements using statistical regression techniques. These methods establish the relationship between brightness temperature with a model or reference soil moisture database. Some regression models are derived from standard RTE (Al-Yaari et al., 2016a, 2016b, 2017; Saleh et al., 2006b; Schmugge and Jackson 1994; Wigneron et al., 2004), while few models involve either simple linear relationship (Eagleman and Lin 1976; Jackson et al., 1999; Theis et al., 1984), or neural network based procedures (Liu et al., 2002; Rodríguez-Fernández et al., 2015; Santi et al., 2016). Certain methods include the vegetation characteristics (e.g. through NDVI, Microwave Polarization Difference Index – MPDI) in the regression models in order to account for the effect of vegetation (Pellarin et al., 2003a; Rodríguez-Fernández et al., 2015; Teng et al., 1993).

It has been noted that the retrievals made from passive L- and C- bands (even X-band at few locations) are significantly influenced by the RFI. This problem is more prominent in the case of the SMOS mission (Oliva et al., 2016). The experience gained from SMOS sensor aided the SMAP mission in improving both sensor design and measurement processing to tackle the RFI (Mohammed et al., 2016). Efforts are being focused towards nullifying the effect of RFI on soil moisture retrievals (Hu et al., 2017). Additionally, soil moisture retrievals are also affected by dense vegetation (Njoku et al., 2003; Vittucci et al., 2016), frozen soils (De Jeu and Owe 2003), organic content (Bircher et al., 2016), litter (Grant et al., 2007; Schmugge et al., 1988), snow & ice (Pulliainen and Hallikainen 2001; Santi et al., 2012), open water (Jones et al., 2009), mountainous regions (De Jeu et al. 2008) and events of active precipitation (Owe et al., 2001), all situations where further algorithmic advances are needed. In a novel attempt, we have summarized the models and the associated literature to passive microwave soil moisture retrieval research in figure form (Fig. 1), wherein the field is divided into 5 branches, concept development (herein the cited literature prominently contributed to the algorithm aspect of soil moisture retrievals), dielectric mixing model, roughness effects, surface temperature, vegetation effects and atmosphere effects. The literature is sorted into these categories according to the contribution made by a particular work (further details are provided in the figure caption).

3. Retrieval of soil moisture from active microwave sensors

The active microwave instruments, in contrast to passive sensors, transmit their own energy source and measure the response that is reflected from the Earth’s surface. The difference in energy between emitted and reflected microwave radiations is the backscatter coefficient ($\sigma°$). The backscatter coefficient is in general expressed in decibels (dB) (Mo et al., 1984). The retrieval of soil moisture from radar sensors was obtained in the 1970s (Jackson et al., 1981; MacDonald and Waite 1971; Ulaby 1974; Ulaby et al., 1974, 1978; Ulaby and Batlivala 1976), simultaneously with the development of passive microwave sensor retrievals. Active microwave sensors are classified into two categories, *imaging*, and *non-imaging* sensors. Radio detection and ranging (radar) is the most common imaging sensor. Synthetic Aperture Radar (SAR) sensors are the advanced form of the imaging sensors used for remote sensing purposes. Some of the prominent SAR satellites include RADARSAT, ENVISAT, TerraSAR-X, Sentinel-1 and active sensor in the SMAP mission. Scatterometers and altimeters are distinguished as non-imaging sensors where the former is used for wind speed and soil moisture sensing and the latter for height measurements. NASA Scatterometer (NSCCAT), QuikSCAT, ERS Scatterometer, MetOp A/B ASCAT are some of the important scatterometers; TOPEX/Poseidon, Jason-1/2, and Cryosat-2 are a few examples of altimeter satellites.

The backscatter coefficient is a function of physical and electrical properties of the soil surface and the radar characteristics (wavelength, polarization, and incidence angle). Furthermore, in the case of a vegetated soil surface, the backscatter coefficient depends on the amount of radiation reflected from the vegetation as well as the soil layers. Similar to the case of passive sensors, lower microwave frequency (L-band) active radiation penetrates the vegetation that is not too dense – thereby minimizing its effect (Ulaby et al., 1986). In addition, active sensors have the ability to achieve higher spatial resolution than radiometers, which results in soil moisture retrievals at a spatial resolution in the order of

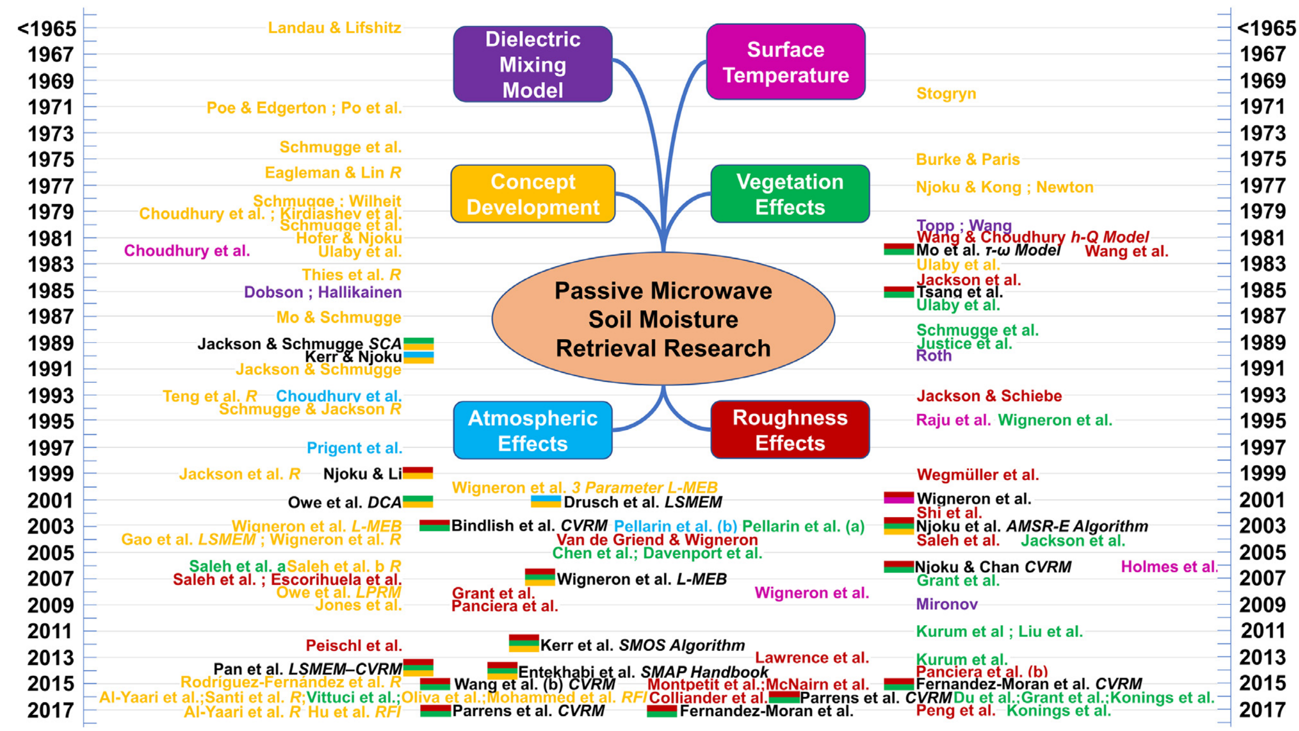

Fig. 1. Summary of the literature and the important developments of the passive microwave soil moisture research. The numbers on the left/right sides indicate the publication year, each of the citations is placed along the line of year during which the work is published. The color of each citation indicates the group to which it belongs. The citations that are shown in black have made multiple contributions, thus belong to multiple groups. The color streaks presented next to these dark colored citations indicate the groups (areas of research) to which the contributions have been made. Few citations are followed by either acronyms or model names (presented in italics), which are either proposed or implemented in the cited work. *CVRM* – Combined vegetation and roughness model; *DCA* – Dual Channel Algorithm; *LPRM* – Land Parameter Retrieval Model; *L-MEB* – L-band Microwave Emission of the Biosphere Model; *LSMEM* - Land Surface Microwave Emission Model; *R* – regression based soil moisture retrieval; *RFI* – Radio Frequency Interference; *SCA* – Single Channel Algorithm.

tens of meters (Walker et al., 2004). However, observations made at such scales have significant effect from surface roughness on the backscatter coefficient (Altese et al., 1996; Liu et al., 2016; Satalino et al., 2002; Wagner et al., 2007). Surface roughness is in general described by root-mean-square (*rms*) height (s), correlation length (L) and Gaussian (or exponential) distributed autocorrelation function (ρ) of surface height (which restricts the roughness characterization to s and L parameters) (Fung et al., 1992; Lievens et al., 2009; Ogilvy and Ogilvy 1991; Ulaby et al., 1996). Furthermore, the sensor configurations such as frequency, polarization and incidence angle also influence the soil moisture and roughness estimates (Baghdadi et al., 2006b, 2013; Rao et al., 1993; Verhoest et al., 2008; Zribi et al., 2014). It is observed that radar signals are more sensitive to soil moisture at low frequencies and low incidence angles (Ulaby et al., 1986). On the other hand, the radar sensitivity to surface roughness increases with increasing incidence angles (Baghdadi et al., 2002a; Fung et al., 1992; Holah et al., 2005; Ulaby et al., 1986; Wang et al., 2015a). Hence, the retrieval algorithm for active sensors should account for these effects and filter them accordingly from backscatter coefficient measured by the sensor to determine the exclusive response from soil moisture (Barrett et al., 2009). Prior to 2002, most active sensors (with an exception of the ERS and the RADARSAT-1 missions), had a mono configuration, which limited the ability to separate the effects of roughness and vegetation from the soil moisture contribution. With ENVISAT that featured multiple polarizations (*HH, VV, HV, VH*) and incidence angles, the ability to separate out the backscatter contribution from the soil surface has improved, resulting in an increase in the soil moisture retrieval accuracy.

The soil moisture retrieval algorithms for active sensors compute the dielectric constant of soil from backscatter coefficients, which is then used to estimate soil moisture (along with other soil properties) using dielectric mixing models (Table 1) (Ulaby et al., 1978). In this way, one can draw parallels between the passive and active sensors' radiative transfer models that the former model simulates brightness temperatures and latter simulates backscatter coefficients with the soil dielectric constant as a primary input. The models used for the retrieval of soil moisture using active sensors can be grouped into four classes: *physical, semi-empirical, empirical* and *change detection* models.

3.1. Physical models

The physical models in active remote sensing of soil moisture simulate backscatter coefficients given primarily the soil dielectric constant, surface roughness and sensor characteristics. In principle, these physical models work similar to RTE of passive microwave systems. The important physical models in this domain are (a) Kirchhoff Approximation (KA) – consisting of the Geometrical Optics Model (GOM) (Stogryn 1967) and Physical Optics Model (POM) (Ulaby et al., 1982); (b) Small Perturbation Model (SPM) (Rice 1951); (c) Small Slope Approximation (SSA) model (Voronovich 1985); and d) Michigan Microwave Canopy Scattering (MIMICS) model (Ulaby et al., 1990). These models are applicable under "specifically" known roughness conditions and the selection of the model depends on the roughness conditions prevailing at the location of interest. A dominant physical model that is developed, based on the above models, is the Integral Equation Model (IEM) (Fung et al., 1992). The IEM simulates the backscatter coefficient as a function of the dielectric constant, sensor parameters, radar frequency (f), polarization, incidence angle (ϑ), *rms* height (s), correlation length (L) and autocorrelation function (ρ):

$$\sigma_{pq}^{o} = \frac{k^2}{2} e^{-2k_z^2 s^2} \sum_{i=1}^{\infty} s^{2i} \left| I_{pq}^{i} \right|^2 \frac{W^{(i)}(-2k_x, 0)}{i!} \tag{7}$$

where, pq is the co-polarization (HH or VV) or cross-polarization (HV or VH); $k = 2\pi f$ is the radar wavenumber; $k_z = k\cos\vartheta, k_x = k\sin\vartheta$; $W^{(i)}(u,v)$is the Fourier transform of ith power of autocorrelation function ρ (which is a function of correlation length L) given by

$$W^{(i)}(u, v) = \frac{1}{2\pi} \iint \rho^i(l, m) e^{(-jul - jvm)} dl dm$$

and

$$I_{pq}^{i} = (2k_z)^i w_{pq} e^{-k_z^2 s^2} + \frac{k_z^i}{2} [F_{pq}(-k_x, 0) + F_{pq}(k_x, 0)] \tag{8}$$

$$\begin{aligned} w_{HH} &= -2R^H / \cos\vartheta \\ w_{VV} &= 2R^V / \cos\vartheta \end{aligned} \tag{9}$$

$$\begin{aligned} &F_{HH}(-k_x, 0) + F_{HH}(k_x, 0) \\ &\quad = -\frac{2\sin^2\vartheta \left(1 + R^H\right)^2}{\cos\vartheta} \left[\left(1 - \frac{1}{\mu_r}\right) + \frac{\mu_r \kappa' - \sin^2\vartheta - \mu_r \cos^2\vartheta}{\mu_r^2 \cos^2\vartheta} \right] \\ &F_{VV}(-k_x, 0) + F_{VV}(k_x, 0) \\ &\quad = -\frac{2\sin^2\vartheta \left(1 + R^V\right)^2}{\cos\vartheta} \left[\left(1 - \frac{1}{\kappa'}\right) + \frac{\mu_r \kappa' - \sin^2\vartheta - \kappa' \cos^2\vartheta}{\kappa'^2 \cos^2\vartheta} \right] \end{aligned} \tag{10}$$

where, κ' is the dielectric constant of the soil (real part); μ_r is the relative permittivity; R^H and R^V are the reflectivities of smooth soil in horizontal and vertical polarizations respectively estimated from the Fresnel's equations (Eq. (2)). The equations for cross polarization conditions can be found in Fung et al., (1992).

The IEM model is applicable only for bare soil conditions due to its inclusion of only single scattering terms that result in surface scattering. Also, the IEM ignores scattering from sub-surface soil layers which could be critical in the case of lower frequencies and dry soil conditions (Schanda 1987). In this regard, the IEM has been modified to include multiple scattering effects (Fung et al., 1996). Subsequently, advancements in the IEM have been introduced by Wu et al. (2001) and Chen et al. (2003) (the evolved model was called the Advanced IEM – AIEM). However, the IEM is difficult to be implemented due to its data requirements. This resulted in the development of “approximation” models – with some models involving empirical calibrations – of the IEM that are applicable for specific frequency and roughness conditions (Rahman et al., 2008). The IEM inversion, on the other hand, relates backscatter coefficients to roughness and soil moisture by fitting the forward IEM simulations with a wide range of soil moisture and roughness conditions through regression or optimization based techniques (Shi et al., 1997). Despite modifications and advancements in the physical model, it is seen that caution must be exercised in implementing the physical models and one cannot generalize their findings made for a specific location to global scales (Bindlish and Barros 2000; Bryant et al., 2007). Also, since roughness conditions are one of the inputs for the physical models that are hard to measure over large regions and given their inherent assumptions, the implementation of IEM could be complicated. This resulted in the development of semi empirical and empirical models.

3.2. Semi-empirical models

Given the difficulties associated with the physical models, the semi-empirical models simplify them to an extent by addressing the issues pertaining to the roughness conditions. These models have the conceptual background of physical models overlaid with simulations or experimental studies that aid in simplification of the models. In the case of IEM, semi-empirical models have been proposed that calibrate the measured roughness effects (particularly the correlation length factor) (Callens and Verhoest 2004; Davidson et al., 2000; Oh and Kay 1998) in order to account for the error between simulated and observed backscatter coefficients (which could arise due to either model or data inconsistencies) (Thoma et al., 2006). In this aspect semi-empirical models involving the calibration of IEM have been developed in the literature (Baghdadi et al., 2002b, 2004, 2006a, 2015; Rahman et al., 2007). The advantage of semi-empirical models is that they can be applicable over any location where the site conditions are within the prescribed limits of the models. Some of the most important semi-empirical models that are widely applied in literature are the methods proposed by Oh et al. (1992) and Dubois et al., (1995).

The Oh et al. (1992) model can be used to estimate volumetric soil moisture (m_V) and roughness by inverting the following relationship between ratios of co-polarized and cross-polarized backscatter coefficients:

$$\begin{aligned} p &= \frac{\sigma_{HH}^{o}}{\sigma_{VV}^{o}} = \left[1 - e^{-ks} \left(\frac{2m_V}{\pi} \right)^{1/3R_o} \right]^2 \\ q &= \frac{\sigma_{HV}^{o}}{\sigma_{VH}^{o}} = 0.23\sqrt{R_o}\left(1 - e^{-ks}\right) \end{aligned} \tag{11}$$

where, p is the co-polarization ratio;ks is the normalized *rms* surface roughness (product of radar wave number and *rms* height); $R_o = |(1 - \sqrt{\kappa'})/(1 + \sqrt{\kappa'})|^2$ is the Fresnel surface reflectivity at the nadir. This model was established using a large database of truck-mounted polarimetric scatterometer measurements, which restricts its application to $0.1 < ks < 6.0$, $2.6 < kl < 19.7$, $0.09 < m_v < 0.31$ and $10° < \vartheta < 70°$, where kl is the normalized correlation length (product of radar wave number and correlation length). The Oh model was further improved to integrate the effects of incidence angle (Oh et al., 1994); to include the full range of surface roughness expected under natural conditions (Oh et al., 2002); and ultimately to ignore the correlation length parameter in the model (Oh, 2004). The advantage of the Oh model lies in its requirement of only one surface parameter (*rms* height – s) for successful soil moisture retrieval. Furthermore, in the case of multi-polarized data, the equations can be used to estimate soil moisture and surface roughness simultaneously without any need for field measurements.

The Dubois model simulates co-polarized backscatter coefficients using the soil dielectric constant (κ') and radar configuration parameters (wavelength – λ; incidence angle – ϑ; wavenumber –k; and surface *rms* height – s):

$$\begin{aligned} \sigma_{HH}^{o} &= 10^{-2.75} \cdot \frac{\cos^{1.5}\vartheta}{\sin^{5.0}\vartheta} \cdot 10^{0.028\kappa' \tan\vartheta} \cdot (ks\sin\vartheta)^{1.4} \cdot \lambda^{0.7} \\ \sigma_{VV}^{o} &= 10^{-2.35} \cdot \frac{\cos^{3.0}\vartheta}{\sin^{3.0}\vartheta} \cdot 10^{0.046\kappa' \tan\vartheta} \cdot (ks\sin\vartheta)^{1.1} \cdot \lambda^{0.7} \end{aligned} \tag{12}$$

These two equations are valid for microwave frequencies in L-, C- and X- bands, $0.3 < s(\text{in}\,cm) < 3$and $30° < \vartheta < 65°$. The model was established using truck mounted scatterometer experiments (Dubois et al., 1995).

Several studies have been carried out to evaluate the performance of semi-empirical and physical models. In the comparisons among the Oh, the Dubois, and the IEM models, Zribi et al. (1997) and Baghdadi et al. (2011) inferred that the IEM performs well over smooth surfaces, and the Oh model simulates backscatter coefficients accurately over rough soils. Choker et al. (2017) compared these three models along with a calibrated IEM using a large database of satellite and in-situ observations and concluded that the latter model is the best-suited model that can be used for soil moisture retrievals. During the evaluation carried out by Panciera et al. (2014a) over Australia, it was found that the IEM, the Oh, and the Dubois models have comparable accuracies under *HH* polarization whereas the Oh model was found to be superior in the case of *VV* polarization. However, Baghdadi and Zribi (2006) have commented that these models either over-estimate or under-estimate backscatter coefficients when evaluated with C-band SAR data.

3.3. Empirical models

Due to the operational limitations of physical and semi-empirical models, several studies have focused on deriving explicit relationships between backscatter coefficients and soil moisture. These studies are limited to the spatio-temporal conditions under which the experiments would have been carried out. Under bare soil conditions, the backscatter coefficient can be related linearly with soil moisture assuming constant roughness and vegetation conditions (Kelly et al., 2003; Lakshmi 2013; Shoshany et al., 2000; Ulaby et al., 1978; Weimann et al., 1998). Few studies also reported non-linearity between soil moisture and the backscatter coefficient (Fung et al., 1992; Narvekar et al., 2015; Paloscia et al., 2013; Tomer et al., 2015; Ulaby et al., 1986). Although there is a linear relationship between soil moisture and backscatter coefficient, the slope and intercept terms vary from site to site (suggesting that the relationship should be calibrated) (Verhoest et al., 2008), which results in the non-applicability of the model that is established for one location to other locations (Baghdadi et al., 2007, 2008a; Le Hégarat-Mascle et al. 2002; Moran et al., 2000; Wang et al., 1986). This relationship is improved by integrating roughness conditions in the form of adding an exponential term to the linear relationship (Baghdadi et al., 2006b, 2007; Zribi and Dechambre 2003). Due to the lack of a physical basis, it is observed that the empirical models are confined to local scale studies. Furthermore, calibrating the empirical models requires good quality in-situ observations of soil moisture as well as roughness parameters (in case of rough soils) which could be an expensive task. Hence, in order to broaden the applicability of empirical models, it is required for the models to include data pertaining to varied conditions of surface roughness and seasons collected over different spatial domains (Baghdadi et al., 2008b).

3.4. Vegetation contribution models

The models described under physical, semi-empirical and empirical approaches are valid only under bare soil conditions. In the case of vegetated soil surfaces, attenuations from vegetation increase with vegetation water content. Hence, one has to account for the contribution of vegetation on backscatter coefficient measured by the active sensor over a vegetated pixel. The effects of vegetation have been addressed by Attema and Ulaby (1978) in their method called the Water-Cloud Model (WCM). This model is semi-empirical by nature because the model parameters are site dependent, which requires calibration (Bindlish and Barros 2001). According to the WCM, the co-polarized backscatter coefficient (σ^o_{pp}) measured at incidence angle ϑcan be expressed as a sum of the backscatter contributions from vegetation; interaction of radar radiation between vegetation and the soil layers; and soil contribution. If the interaction term from co-polarization measurements is neglected (Dobson and Ulaby 1986; Prevot et al., 1993), the WCM can be expressed by the following equation:

$$\sigma^o_{pp} = \sigma^o_{veg} + \delta^2 \sigma^o_{soil} \tag{13}$$

with,

$$\begin{aligned} \sigma^o_{veg} &= A \cdot V_1 \cdot \cos\vartheta \cdot \left(1 - \delta^2\right) \\ \delta &= \exp\left(-2BV_2 \sec\vartheta\right) \\ \sigma^o_{soil} &= C + D \cdot m_v \end{aligned} \tag{14}$$

where, σ^o_{veg} and σ^o_{soil} are the backscatter contributions from vegetation and soil respectively; δ^2 is the two-way vegetation attenuation; V_1 and V_2 are the vegetation descriptors, which according to Bindlish and Barros (2001) are equivalent to the Vegetation Water Content (*VWC*) that can be estimated from ancillary sources (as described in Section 2); and *A, B, C, D* are the vegetation and soil parameters which need to be calibrated according to the location of interest. An alternative vegetation correction method called the ‘ratio’ method was later proposed by Joseph et al., (2008, 2010). This method considers that the ratio of bare soil contribution to the backscatter coefficient (σ^o_{soil}), and the observed backscatter coefficient (σ^o_{pp}) is a function of vegetation cover (represented by the *VWC*) and sensor configuration. The initial model proposed by Joseph et al. (2008) has the following functional relationship with *a* and *b* as calibration parameters. In their study, Joseph et al. (2010), it was found that the ratio method, despite the simplicity, is sufficient to quantify the contribution of vegetation in soil moisture retrievals. Several works have coupled the WCM with active retrieval algorithms to obtain soil moisture (Bai et al., 2017; Hosseini and McNairn 2017; Liu and Shi 2016).

$$\frac{\sigma^o_{soil}}{\sigma^o_{pp}} = a \cdot VWC^2 + e^{-b \cdot VWC} \tag{15}$$

Zribi et al. (2003) proposed an empirical technique of estimating the vegetation contribution to the measured backscatter coefficient. Consider a portion of pixel that is covered with forest where the radar signal cannot penetrate the canopy structure. The contribution of backscatter from the non-forested portion (σ^o_{others}) of the pixel is estimated by factoring it with the forest area (A_{forest}) in the pixel ($\sigma^o_{others} = (\sigma^o_{pp} - A_{forest} \cdot \sigma^o_{forest})/(1 - A_{forest})$), and the backscatter contribution from the forest (σ^o_{forest}) can be estimated from a functional relationship with the incidence angle (ϑ) and time (t) of the year (which indicates seasonal growth) (Zribi et al., 2003) using the following relationship with *A, B, D, E* as calibration parameters.

$$\sigma^o_{forest} = D\vartheta + E + A\sin\left[\frac{2\pi}{12}t + B\right] \tag{16}$$

3.5. Change detection approach

While the physical, semi-empirical and empirical models rely on backscatter coefficient information obtained in a single time period, it was noticed that the data from multi-temporal passes made by an active sensor at a location can be used to obtain the relative change in soil moisture (if not its absolute value) at that location (Engman 1994). If the roughness and vegetation conditions are assumed to be time invariant, or vary at time scales much longer than that of soil moisture, it can be assumed that the change in backscatter coefficient between two different time periods is exclusively due to the change in soil moisture conditions (Moran et al., 2004). Based on this assumption, several change detection methods have been proposed, which represent change as difference (e.g. delta index approach (Thoma et al., 2004, 2006)) or as a ratio (e.g. alpha approximation method (Balenzano et al., 2011) and its extensions (He et al., 2017; Ouellette et al., 2017)), to retrieve relative soil moisture levels using active microwave observations. Given backscatter coefficients of a location at two times (t_1 and t_2), Shoshany et al., (2000) introduced the normalized radar backscatter soil moisture index (*NBMI*) (Eq. (17)) to calculate relative soil moisture (values ranging between 0 and 1) at that location.

$$NBMI = \frac{\sigma^o_{t_1} - \sigma^o_{t_2}}{\sigma^o_{t_1} + \sigma^o_{t_2}} \tag{17}$$

In another approach of change detection developed in the works of Wagner (1998), Wagner et al., (1999a, 1999b), and Wagner and Scipal (2000), the relative soil moisture on a particular day t (SM_t) is estimated by comparing backscatter coefficient with dry and wet backscatter conditions (all of which are measured at the reference angle ϑ_{ref}).

$$SM_t = \frac{\sigma^o\left(t, \vartheta_{ref}\right) - \sigma^o_{dry}\left(t, \vartheta_{ref}\right)}{\sigma^o_{wet}\left(t, \vartheta_{ref}\right) - \sigma^o_{dry}\left(t, \vartheta_{ref}\right)} \times 100 \tag{18}$$

where, $\sigma^o(t,\vartheta_{ref})$ is the backscatter coefficient measured on day t with reference angle ϑ_{ref}; $\sigma^o_{dry}(t, \vartheta_{ref})$ and $\sigma^o_{wet}(t, \vartheta_{ref})$ are the historically lowest (representing driest conditions) and highest (representing wettest conditions) values of backscatter coefficients respectively observed on day t of the year with reference angle ϑ_{ref} obtained from long backscatter time series of the location under study. Such a normalization accounts for roughness and vegetation conditions (Wagner et al., 1999a). The obtained relative soil moisture is the degree of saturation of the soil layer expressed in %. This methodology, which in general is called the TU-Wien change detection algorithm, is used in the Soil Water Retrieval Package (WARP) algorithm to obtain soil moisture retrievals from the Advanced Scatterometer (ASCAT) sensors onboard the MetOp-A and MetOp-B satellites (Bartalis et al., 2007; Naeimi et al., 2009a, 2009b). This retrieval algorithm filters for frozen soil and snow cover as well. Further details regarding change detection based retrieval algorithms can be obtained from Barrett et al., (2009). Attempts are now being made to improve the components of this retrieval algorithm in terms of addressing outliers in the computation of $\sigma^o_{dry}(t, \vartheta_{ref})$ and $\sigma^o_{wet}(t, \vartheta_{ref})$ (Naeimi et al., 2009b); vegetation characterization (Vreugdenhil et al., 2016); and incidence angle dependence (Hahn et al., 2017). A summary of models and the associated literature for active microwave soil moisture retrieval research is presented in Fig. 2, wherein the field is divided into 5 categories, soil moisture/vegetation/roughness characterization (herein the cited literature prominently contributed towards characterizing either soil moisture or roughness or vegetation in the perspective of active microwave remote sensing), physical models, semi-empirical models, empirical models and change detection approach. The literature is sorted into these categories according to the contribution made by a particular work (further details are provided in the figure caption).

4. Discussion & conclusions

This review provides a comprehensive overview of the retrieval algorithms used in processing the data from passive and active microwave sensors for estimating soil moisture. We looked at how microwave sensors have evolved over time to address the growing need to estimate the soil moisture accurately at global scales. Since retrieval algorithms play a key role in retrieving soil moisture from space-borne sensor measurements, we tried to summarize the important findings of their evolution.

4.1. Passive microwave retrieval algorithms

All of the passive microwave retrieval algorithms are based on the zeroth order radiative transfer equation. In the case of the SMOS algorithm, due to the complicated Y-shaped design of the sensor, separate models have to be employed to address the effects of forests, litter, dry sand, and open water. Given what was learned from the SMOS mission, the SMAP mission followed a relatively more conservative sensor design (with extra effort on RFI issues) and a 'straightforward' Single Channel Algorithm (SCA) resulting in substantial improvements in the accuracy of SMAP's soil moisture retrievals (the results of which are presented in part 2 of this review). This suggests that dedicated soil moisture missions and simpler models can help reduce the uncertainty arising in the retrieval process.

The contribution of roughness to passive microwave emissions is in general quantified using Wang and Choudhury (1981)'s *h*-*Q* model with some variations. For example, LPRM and LSMEM assume constant values of these parameters, whereas SMAP's algorithm uses the land cover dependent h parameter (with $Q = 0$). In this regard, further research is needed to evaluate the rationale behind the formulation of a roughness model for a particular sensor. The roughness can be influenced by soil type and seasonal climatic changes that are not considered in the current retrieval algorithms. This could affect the spatial pattern and the seasonal cycle of soil moisture retrievals. If these impacts are deemed to be significant, there will be a need to develop a dynamic global roughness map, which accounts for variations in space and time.

The contribution from the vegetation layer is addressed using the $\tau - \omega$ model. The current soil moisture missions, SMOS, and SMAP, rely on the ancillary optical observations (e.g. NDVI) to estimate the vegetation optical depth (τ), whereas the algorithms such as LPRM and LSMEM retrieve simultaneously the vegetation optical depth and soil moisture using only microwave measurements. Both the techniques have pros and cons. Accuracy of ancillary data, inconsistency in its temporal and spatial resolutions from those of a microwave sensor, and the process of relating the ancillary variable with the vegetation optical depth can influence the quality of soil moisture retrievals. The simultaneously retrieved vegetation optical depth, in general, depicts higher temporal variability than expected, which may contribute to noise in soil moisture retrievals. Since the emissions from the soil layer are significantly attenuated in the dense vegetation regions, the possibility of considering multiple scatter effects should be explored for these areas to better resolve the contribution from the soil layer beneath the vegetation.

4.2. Active microwave retrieval algorithms

For active sensors, the soil roughness is the dominant contributor to the measured radar backscatter coefficients alongside soil moisture content in the case of bare soils. The soil moisture retrievals are also influenced by sensor configurations like the operating frequency, polarization, and incidence angle. Hence, the retrieval algorithms attempt to address these effects simultaneously, which still remains a challenge at global scales. The physical models such as the Integral Equation Model (IEM), developed for estimating the roughness and the soil moisture from radar measurements are found to be complex in nature and data intensive, making them too demanding for operational implementation. The semi-empirical models, such as the Oh and the Dubois models, are widely-used algorithms which, to a certain extent, reduce the complexity and data requirement of physical models. Both types of retrieval algorithms have their own strengths and limitations in terms of physical consistency, universal applicability, performance, manageability, and efficiency.

In the case of active remote sensing over vegetated areas, the physical models should be used in tandem with methods such as the Water-Cloud Model (WCM) and the 'ratio' model that separate the backscatter contribution of vegetation from total backscatter recorded by the sensor. These models require ancillary information of the vegetation water content, which, similar to passive microwave algorithms, is derived from ancillary optical datasets. Due to the involvement of empirical parameters in physical models of

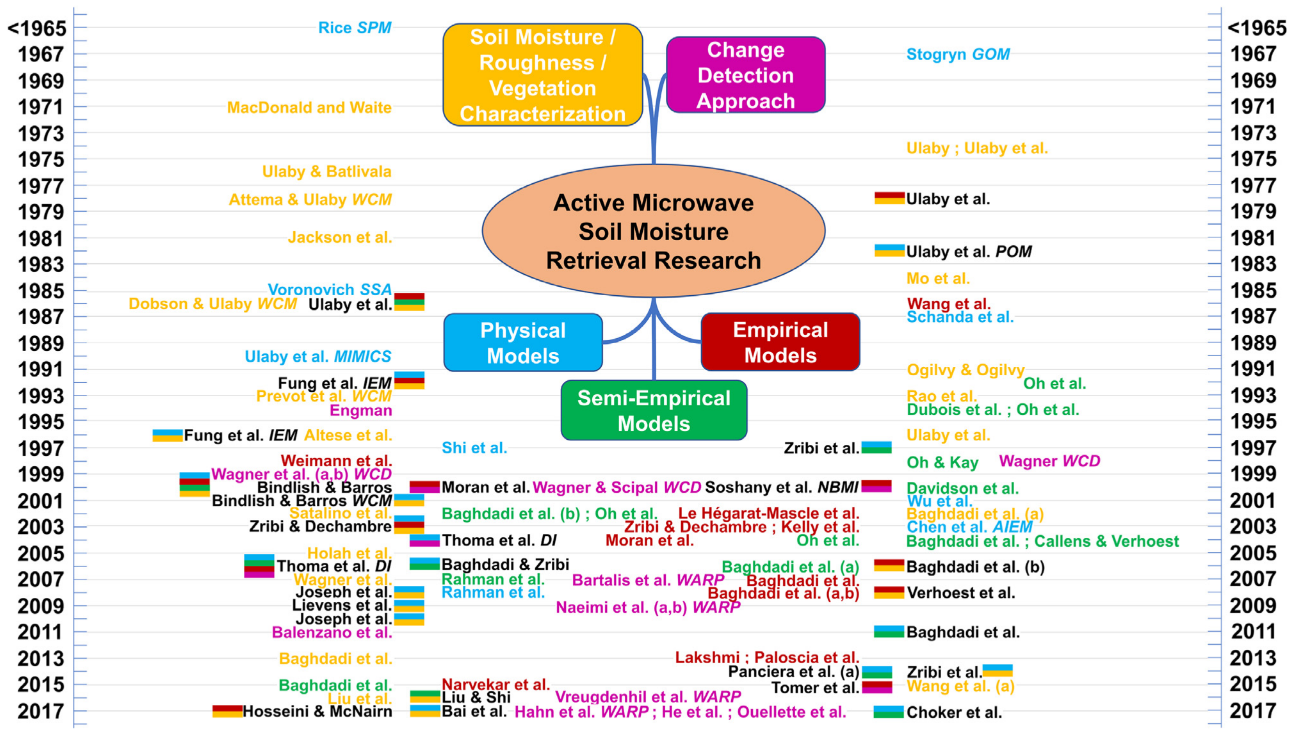

Fig. 2. Summary of the literature and the important developments of the active microwave soil moisture research. The numbers on the left/right sides indicate the publication year, each of the citations is placed along the line of year during which the work is published. The color of each citation indicates the group to which it belongs. The citations that are shown in black have made multiple contributions, thus belong to multiple groups. The color streaks presented next to these dark colored citations indicate the groups (areas of research) to which the contributions have been made. Few citations are followed by either acronyms or model names (presented in italics), which are either proposed or implemented in the cited work. *AIEM* – Advanced Integral Equation Model; *DI* – Delta Index approach; *GOM* – Geometrical Optics Model; *IEM* – Integral Equation Model; *MIMICS* – Michigan Microwave Canopy Scattering model; *POM* – Physical Optics Model; *SPM* – Standard Perturbation Model; *SSA* – Small Slope Approximation model; *WARP* – Soil Water Retrieval Package; *WCD* – TU-Wien change detection algorithm; *WCM* – Water Cloud Model.

bare soil and vegetation, which need to be calibrated per location, it is still difficult to implement them at global scales.

The change detection algorithm tries to overcome the limitations of physical models by primarily assuming that the roughness conditions remain constant over time at a location so that the temporal changes in the backscatter coefficient are attributed to relative changes in soil moisture. This method not only eliminates the need for the calibration of empirical parameters but also facilitates global scale soil moisture retrieval through an active sensor. The active soil moisture products that use a change detection algorithm achieved reasonable temporal and spatial accuracy during their validation (presented in Part 2) over the Contiguous United States (CONUS) region.

4.3. Dielectric mixing models

There is no clear consensus regarding the selection of a dielectric mixing model for both passive and active microwave soil moisture retrieval algorithms (if physical retrieval models are used). Also, the effect of empirical factors in these models on the quality of soil moisture retrievals is not investigated. Hence, a thorough sensitivity analysis may be needed to find out how different dielectric mixing parameterizations can affect different physical retrieval models in terms of uncertainty and retrieval performance. This analysis should help identifying the dielectric mixing models that work best with a particular physical model.

5. Future challenges

Various challenges have been identified and put forward by the soil moisture remote sensing community over the past decades in terms of the underlying physics and retrieval approaches. The following fields are identified in this review that need further efforts:

- There is a need to further resolve the physical underpinnings of many empirical parameters (e.g. soil roughness and vegetation albedo) in the retrieval algorithms in order to improve their global applicability and to estimate additional physical variables (e.g. plant biophysical variables).
- It is necessary to estimate the sensitivity of soil moisture retrievals from a single sensor with multiple algorithms, to gain a further understanding of the algorithm uncertainty and sensitivity. Currently, the retrievals from AMSR-E with LPRM and LSMEM algorithms is one example.
- Better vegetation optical depth (VOD) retrieval algorithms are necessary to facilitate soil moisture retrievals for the densely-vegetated regions.
- The applicability of physics based models of active microwave algorithms should be expanded to global scale with ease in their implementation.
- Errors in soil moisture products are the result of noise due to the sensor (e.g. removal of Faraday rotation effect) and algorithm. Efforts are needed to identify the source and impact of various noise/uncertainty sources, with efforts directed towards developing algorithms to reduce/eliminate noise and handle uncertainties so as to improve retrieval quality.
- The operational dielectric mixing models such as the Dobson model and the Wang and Schmugge model have not been revisited since 1980s. Thus, a larger database of recent soil samples may help to improve the mixing model and to reduce model uncertainty in soil moisture retrievals of operational missions.

Acknowledgments

The work reported in this paper was done while the first author was a visiting scholar at Princeton University under the Fulbright-Nehru India Doctoral Research program (Grant Id: 15160292). Additional support for the research is from NASA Grants NNX14AH92G (Soil Moisture Cal/Val Activities as a SMAP Mission Science Team Member) and NNX13AI44G (Developing a statistical-physical integrated approach for downscaling hydrologic information from GCM), and NWO Rubicon 825.15.003. The support from these programs is gratefully acknowledged.

References

Al-Yaari, A., Wigneron, J.-P., Kerr, Y., Rodriguez-Fernandez, N., O'Neill, P., Jackson, T., De Lannoy, G., Al Bitar, A., Mialon, A., Richaume, P., 2016a. First application of regression analysis to retrieve Soil Moisture from SMAP brightness temperature observations consistent with SMOS. In: Proceedings of the 2016 IEEE International Geoscience and Remote Sensing Symposium (IGARSS), pp. 1633–1636. IEEE.
Al-Yaari, A., Wigneron, J., Kerr, Y., De Jeu, R., Rodriguez-Fernandez, N., Van Der Schalie, R., Al Bitar, A, Mialon, A., Richaume, P., Dolman, A., 2016b. Testing regression equations to derive long-term global soil moisture datasets from passive microwave observations. Remote Sens. Environ. 180, 453–464.
Al-Yaari, A., Wigneron, J.-P., Kerr, Y., Rodriguez-Fernandez, N., O'Neill, P., Jackson, T., De Lannoy, G., Al Bitar, A., Mialon, A., Richaume, P., 2017. Evaluating soil moisture retrievals from ESA's SMOS and NASA's SMAP brightness temperature datasets. Remote Sens. Environ. 193, 257–273.
Altese, E., Bolognani, O., Mancini, M., Troch, P.A., 1996. Retrieving soil moisture over bare soil from ERS 1 synthetic aperture radar data: Sensitivity analysis based on a theoretical surface scattering model and field data. Water Resourc. Res. 32, 653–661.
Alvarez-Garreton, C., Ryu, D., Western, A., Su, C.-H., Crow, W., Robertson, D., Leahy, C., 2015. Improving operational flood ensemble prediction by the assimilation of satellite soil moisture: comparison between lumped and semi-distributed schemes. Hydrol. Earth Syst. Sci. 19, 1659–1676.
Attema, E., Ulaby, F.T., 1978. Vegetation modeled as a water cloud. Radio Sci. 13, 357–364.
Baghdadi, N., Aubert, M., Cerdan, O., Franchistéguy, L., Viel, C., Eric, M., Zribi, M., Desprats, J.F., 2007. Operational mapping of soil moisture using synthetic aperture radar data: application to the Touch basin (France). Sensors 7, 2458–2483.
Baghdadi, N., Cerdan, O., Zribi, M., Auzet, V., Darboux, F., El Hajj, M., Kheir, R.B., 2008a. Operational performance of current synthetic aperture radar sensors in mapping soil surface characteristics in agricultural environments: application to hydrological and erosion modelling. Hydrol. Process. 22, 9–20.
Baghdadi, N., Dubois-Fernandez, P., Dupuis, X., Zribi, M., 2013. Sensitivity of main polarimetric parameters of multifrequency polarimetric SAR data to soil moisture and surface roughness over bare agricultural soils. IEEE Geosci. Remote Sens. Lett. 10, 731–735.
Baghdadi, N., Gherboudj, I., Zribi, M., Sahebi, M., King, C., Bonn, F., 2004. Semi-empirical calibration of the IEM backscattering model using radar images and moisture and roughness field measurements. Int. J. Remote Sens. 25, 3593–3623.
Baghdadi, N., Holah, N., Zribi, M., 2006a. Calibration of the integral equation model for SAR data in C-band and HH and VV polarizations. Int. J. Remote Sens. 27, 805–816.
Baghdadi, N., Holah, N., Zribi, M., 2006b. Soil moisture estimation using multi-incidence and multi-polarization ASAR data. Int. J. Remote Sens. 27, 1907–1920.
Baghdadi, N., King, C., Bourguignon, A., Remond, A., 2002a. Potential of ERS and RADARSAT data for surface roughness monitoring over bare agricultural fields: application to catchments in Northern France. Int. J. Remote Sens. 23, 3427–3442.
Baghdadi, N., King, C., Chanzy, A., Wigneron, J., 2002b. An empirical calibration of the integral equation model based on SAR data, soil moisture and surface roughness measurement over bare soils. Int. J. Remote Sens. 23, 4325–4340.
Baghdadi, N., Saba, E., Aubert, M., Zribi, M., Baup, F., 2011. Evaluation of radar backscattering models IEM, Oh, and Dubois for SAR data in X-band over bare soils. IEEE Geosci. Remote Sens. Lett. 8, 1160–1164.
Baghdadi, N., Zribi, M., 2006. Evaluation of radar backscatter models IEM, OH and Dubois using experimental observations. Int. J. Remote Sens. 27, 3831–3852.
Baghdadi, N., Zribi, M., Loumagne, C., Ansart, P., Anguela, T.P., 2008b. Analysis of TerraSAR-X data and their sensitivity to soil surface parameters over bare agricultural fields. Remote Sens. Environ. 112, 4370–4379.
Baghdadi, N., Zribi, M., Paloscia, S., Verhoest, N.E., Lievens, H., Baup, F., Mattia, F., 2015. Semi-empirical calibration of the integral equation model for co-polarized L-band backscattering. Remote Sens. 7, 13626–13640.
Bai, X., He, B., Li, X., Zeng, J., Wang, X., Wang, Z., Zeng, Y., Su, Z., 2017. First assessment of sentinel-1A data for surface soil moisture estimations using a coupled water cloud model and advanced integral equation model over the Tibetan plateau. Remote Sens. 9, 714.
Baldwin, D., Manfreda, S., Keller, K., Smithwick, E., 2017. Predicting root zone soil moisture with soil properties and satellite near-surface moisture data across the conterminous United States. J. Hydrol. 546, 393–404.
Balenzano, A., Mattia, F., Satalino, G., Davidson, M.W., 2011. Dense temporal series of C-and L-band SAR data for soil moisture retrieval over agricultural crops. IEEE J. Selected Top. Appl. Earth Observ. Remote Sens. 4, 439–450.
Barrett, B.W., Dwyer, E., Whelan, P., 2009. Soil moisture retrieval from active spaceborne microwave observations: An evaluation of current techniques. Remote Sens. 1, 210–242.
Bartalis, Z., Wagner, W., Naeimi, V., Hasenauer, S., Scipal, K., Bonekamp, H., Figa, J., Anderson, C., 2007. Initial soil moisture retrievals from the METOP-A Advanced Scatterometer (ASCAT). Geophys. Res. Lett. 34.
Berg, A., Lintner, B., Findell, K., Giannini, A., 2017. Soil moisture influence on seasonality and large-scale circulation in simulations of the West African Monsoon. J. Climate 30, 2295–2317.
Berg, A., Lintner, B.R., Findell, K.L., Malyshev, S., Loikith, P.C., Gentine, P., 2014. Impact of soil moisture–atmosphere interactions on surface temperature distribution. J. Climate 27, 7976–7993.
Bindlish, R., Barros, A.P., 2000. Multifrequency soil moisture inversion from SAR measurements with the use of IEM. Remote Sens. Environ. 71, 67–88.
Bindlish, R., Barros, A.P., 2001. Parameterization of vegetation backscatter in radar-based, soil moisture estimation. Remote Sens. Environ. 76, 130–137.
Bindlish, R., Jackson, T.J., Wood, E., Gao, H., Starks, P., Bosch, D., Lakshmi, V., 2003. Soil moisture estimates from TRMM Microwave Imager observations over the Southern United States. Remote Sens. Environ. 85, 507–515.
Bircher, S., Andreasen, M., Vuollet, J., Vehviläinen, J., Rautiainen, K., Jonard, F., Weihermüller, L., Zakharova, E., Wigneron, J., Kerr, Y., 2016. Soil moisture sensor calibration for organic soil surface layers. Geosci. Instrum. Methods Data Syst. 5, 109–125.
Blinn, J.C., Quade, J.G., 1972. Microwave properties of geological materials: Studies of penetration depth and moisture effects. In, 4th Annual Earth Resources Program Review, NASA. Lyndon B. Johnson Space Center, Houston, Texas, USA.
Bolten, J.D., Crow, W.T., Zhan, X., Jackson, T.J., Reynolds, C.A., 2010. Evaluating the utility of remotely sensed soil moisture retrievals for operational agricultural drought monitoring. IEEE J. Selected Top. Appl. Earth Observ. Remote Sens. 3, 57–66.
Bryant, R., Moran, M.S., Thoma, D., Collins, C.H., Skirvin, S., Rahman, M., Slocum, K., Starks, P., Bosch, D., Dugo, M.G., 2007. Measuring surface roughness height to parameterize radar backscatter models for retrieval of surface soil moisture. IEEE Geosci. Remote Sens. Lett. 4, 137–141.
Burke, W., Paris, J.F., 1975. A radiative transfer model for microwave emissions from bare agricultural soils. NASA–TM–X–58166, JSC–09836. Houston, TX, United States: NASA Johnson Space Center.
Burke, W., Schmugge, T., Paris, J., 1979. Comparison of 2.8-and 21-cm microwave radiometer observations over soils with emission model calculations. J. Geophys. Res. Oceans, 84, 287–294.
Callens, M., Verhoest, N., 2004. Description and Analysis of the Soil Roughness Field Campaign Conducted at the Experimental Farm of Ghent University During the Winter Period 2002–2003. Laboratory of Hydrology and Water Management, Ghent University.
Calvet, J.-C., Wigneron, J.-P., Walker, J., Karbou, F., Chanzy, A., Albergel, C., 2011. Sensitivity of passive microwave observations to soil moisture and vegetation water content: L-band to W-band. IEEE Trans. Geosci. Remote Sens. 49, 1190–1199.
Chan, S.K., Bindlish, R., O'Neill, P.E., Njoku, E., Jackson, T., Colliander, A., Chen, F., Burgin, M., Dunbar, S., Piepmeier, J., 2016. Assessment of the SMAP passive soil moisture product. IEEE Trans. Geosci. Remote Sens. 54, 4994–5007.
Chen, D., Huang, J., Jackson, T.J., 2005. Vegetation water content estimation for corn and soybeans using spectral indices derived from MODIS near-and short-wave infrared bands. Remote Sens. Environ. 98, 225–236.
Chen, K.-S., Wu, T.-D., Tsang, L., Li, Q., Shi, J., Fung, A.K., 2003. Emission of rough surfaces calculated by the integral equation method with comparison to three--dimensional moment method simulations. IEEE Trans. Geosci. Remote Sens. 41, 90–101.
Choker, M., Baghdadi, N., Zribi, M., Hajj, El, M., Paloscia, S., Verhoest, N.E., Lievens, H, Mattia, F., 2017. Evaluation of the Oh, Dubois and IEM Backscatter Models Using a Large Dataset of SAR Data and Experimental Soil Measurements. Water, 9, 38.
Choudhury, B., Schmugge, T., Mo, T., 1982. A parameterization of effective soil temperature for microwave emission. J. Geophys. Res. Oceans 87, 1301–1304.
Choudhury, B., Schmugge, T.J., Chang, A., Newton, R., 1979. Effect of surface roughness on the microwave emission from soils. J. Geophys. Res. Oceans 84, 5699–5706.
Choudhury, B.J., 1993. Reflectivities of selected land surface types at 19 and 37 GHz from SSM/I observations. Remote Sens. Environ. 46, 1–17.
Colliander, A., Njoku, E.G., Jackson, T.J., Chazanoff, S., McNairn, H., Powers, J., Cosh, M.H., 2016. Retrieving soil moisture for non-forested areas using PALS radiometer measurements in SMAPVEX12 field campaign. Remote Sens. Environ. 184, 86–100.
Das, N., Mohanty, B., Cosh, M., Jackson, T., 2008. Modeling and assimilation of root zone soil moisture using remote sensing observations in Walnut Gulch Watershed during SMEX04. Remote Sens. Environ. 112, 415–429.
Davenport, I.J., Fernández-Gálvez, J., Gurney, R.J., 2005. A sensitivity analysis of soil moisture retrieval from the tau-omega microwave emission model. IEEE Trans. Geosci. Remote Sens., 43, 1304–1316.
Davidson, M.W., Le Toan, T., Mattia, F., Satalino, G., Manninen, T., Borgeaud, M., 2000. On the characterization of agricultural soil roughness for radar remote sensing studies. IEEE Trans. Geosci. Remote Sens., 38, 630–640.
De Jeu, R., Owe, M., 2003. Further validation of a new methodology for surface moisture and vegetation optical depth retrieval. Int. J. Remote Sens. 24, 4559–4578.

De Jeu, R., Wagner, W., Holmes, T., Dolman, A., Van De Giesen, N., Friesen, J., 2008. Global soil moisture patterns observed by space borne microwave radiometers and scatterometers. Surv. Geophys. 29, 399–420.
Dobson, M.C., Ulaby, F.T., 1986. Active microwave soil moisture research. IEEE Trans. Geosci. Remote Sens. 23–36.
Dobson, M.C., Ulaby, F.T., Hallikainen, M.T., El-Rayes, M.A., 1985. Microwave dielectric behavior of wet soil-Part II: Dielectric mixing models. IEEE Trans. Geosci. Remote Sens. 35–46.
Drusch, M., Wood, E.F., Jackson, T.J., 2001. Vegetative and atmospheric corrections for the soil moisture retrieval from passive microwave remote sensing data: Results from the Southern Great Plains Hydrology Experiment 1997. J. Hydrometeorol. 2, 181–192.
Drusch, M., Scipal, K., De Rosnay, P., Balsamo, G., Andersson, E., Bougeault, P., Viterbo, P., 2009. Towards a Kalman Filter based soil moisture analysis system for the operational ECMWF Integrated Forecast System. Geophys. Res. Lett. 36.
Du, J., Kimball, J.S., Jones, L.A., 2016. Passive microwave remote sensing of soil moisture based on dynamic vegetation scattering properties for AMSR-E. IEEE Trans. Geosci. Remote Sens., 54, 597–608.
Dubois, P.C., Van Zyl, J., Engman, T., 1995. Measuring soil moisture with imaging radars. *IEEE Trans. Geosci. Remote Sens.*, 33, 915–926.
Dumedah, G., Walker, J.P., Merlin, O., 2015. Root-zone soil moisture estimation from assimilation of downscaled Soil Moisture and Ocean Salinity data. Adv. Water Resour. 84, 14–22.
Eagleman, J.R., Lin, W.C., 1976. Remote sensing of soil moisture by a 21-cm passive radiometer. J. Geophys. Res. 81, 3660–3666.
Engman, E.T., 1994. The potential of SAR in hydrology. In: Proceedings of the International Geoscience and Remote Sensing Symposium, 1994. IGARSS'94. Surface and Atmospheric Remote Sensing: Technologies, Data Analysis and Interpretation, pp. 283–285. IEEE.
Entekhabi, D., Yueh, S., O'Neill, P., Kellogg, K., Allen, A., Bindlish, R., Brown, M., Chan, S., Colliander, A., Crow, W., 2014. In: SMAP Handbook, 182. JPL Publication JPL, Pasadena, California, pp. 400–1567.
Escorihuela, M.J., Kerr, Y.H., de Rosnay, P., Wigneron, J.-P., Calvet, J.-C., Lemaitre, F., 2007. A simple model of the bare soil microwave emission at L-band. IEEE Trans. Geosci. Remote Sens. 45, 1978–1987.
Fernandez-Moran, R., Wigneron, J.-P., Lopez-Baeza, E., Al-Yaari, A., Coll-Pajaron, A., Mialon, A., Miernecki, M., Parrens, M., Salgado-Hernanz, P., Schwank, M., 2015. Roughness and vegetation parameterizations at L-band for soil moisture retrievals over a vineyard field. Remote Sens. Environ. 170, 269–279.
Fernandez-Moran, R., Wigneron, J.-P., De Lannoy, G., Lopez-Baeza, E., Parrens, M., Mialon, A., Mahmoodi, A., Al-Yaari, A., Bircher, S., Al Bitar, A., 2017. A new calibration of the effective scattering albedo and soil roughness parameters in the SMOS SM retrieval algorithm. Int. J. Appl. Earth Observ. Geoinform. 62, 27–38.
Fung, A., Dawson, M., Chen, K., Hsu, A., Engman, E., O'Neill, P., Wang, J., 1996. A modified IEM model for: scattering from soil surfaces with application to soil moisture sensing. In: Proceedings of the International Geoscience and Remote Sensing Symposium, 1996. IGARSS'96.'Remote Sensing for a Sustainable Future', pp. 1297–1299. IEEE.
Fung, A.K., Li, Z., Chen, K.-S., 1992. Backscattering from a randomly rough dielectric surface. IEEE Trans. Geosci. Remote Sens. 30, 356–369.
Gao, H., Wood, E.F., Drusch, M., Crow, W., Jackson, T.J., 2004. Using a microwave emission model to estimate soil moisture from ESTAR observations during SGP99. J. Hydrometeorol. 5, 49–63.
Grant, J., Wigneron, J.-P., De Jeu, R., Lawrence, H., Mialon, A., Richaume, P., Al Bitar, A., Drusch, M., van Marle, M., Kerr, Y., 2016. Comparison of SMOS and AMSR-E vegetation optical depth to four MODIS-based vegetation indices. Remote Sens. Environ. 172, 87–100.
Grant, J., Wigneron, J.-P., Van de Griend, A., Kruszewski, A., Søbjærg, S.S., Skou, N., 2007. A field experiment on microwave forest radiometry: L-band signal behaviour for varying conditions of surface wetness. Remote Sens. Environ. 109, 10–19.
Grant, J.P., Saleh-Contell, K., Wigneron, J.-P., Guglielmetti, M., Kerr, Y.H., Schwank, M., Skou, N., Van de Griend, A.A., 2008. Calibration of the L-MEB model over a coniferous and a deciduous forest. IEEE Trans. Geosci. Remote Sens. 46, 808–818.
Hahn, S., Reimer, C., Vreugdenhil, M., Melzer, T., Wagner, W., 2017. Dynamic characterization of the incidence angle dependence of backscatter using metop ASCAT. IEEE J. Select. Top. Appl. Earth Observ. Remote Sens.
Hallikainen, M.T., Ulaby, F.T., Dobson, M.C., El-Rayes, M.A., Wu, L.-K., 1985. Microwave dielectric behavior of wet soil-part 1: Empirical models and experimental observations. IEEE Trans. Geosci. Remote Sens. 25–34.
He, L., Qin, Q., Panciera, R., Tanase, M., Walker, J.P., Hong, Y., 2017. An extension of the alpha approximation method for soil moisture estimation using time-Series SAR data over bare soil surfaces. IEEE Geosci. Remote Sens. Lett.
Hofer, R., Njoku, E.G., 1981. Regression techniques for oceanographic parameter retrieval using space-borne microwave radiometry. IEEE Trans. Geosci. Remote Sens. 178–189.
Holah, N., Baghdadi, N., Zribi, M., Bruand, A., King, C., 2005. Potential of ASAR/ENVISAT for the characterization of soil surface parameters over bare agricultural fields. Remote Sens. Environ. 96, 78–86.
Holmes, T., De Rosnay, P., De Jeu, R., Wigneron, R.P., Kerr, Y., Calvet, J.C., Escorihuela, M., Saleh, K., Lemaître, F., 2006. A new parameterization of the effective temperature for L band radiometry. Geophys. Res. Lett. 33.
Hosseini, M., McNairn, H., 2017. Using multi-polarization C-and L-band synthetic aperture radar to estimate biomass and soil moisture of wheat fields. Int. J. Appl. Earth Observ. Geoinform. 58, 50–64.
Hu, F., Peng, X., He, F., Wu, L., Li, J., Cheng, Y., Zhu, D., 2017. RFI mitigation in aperture synthesis radiometers using a modified CLEAN algorithm. IEEE Geosci. Remote Sens. Lett. 14, 13–17.
Jackson, T., Chang, A., Schmugge, T., 1981. Aircraft active microwave measurements for estimating soil moisture. Photogram. Eng. Remote Sens. 47, 801–805.
Jackson, T., Schiebe, F., 1993. Washita '92 data report. In: Jackson, T., Schiebe, F. (Eds.), NAWQL Report 101, Eds. USDA National Agricultural Water Quality Lab, Durant OK.
Jackson, T., Schmugge, T., 1989. Algorithm for the passive microwave remote sensing of soil moisture. Microwave Radiom. Remote Sens. Appl. 3–17.
Jackson, T., Schmugge, T., 1991. Vegetation effects on the microwave emission of soils. Remote Sens. Environ. 36, 203–212.
Jackson, T., Schmugge, T., O'Neill, P., 1984. Passive microwave remote sensing of soil moisture from an aircraft platform. Remote Sens. Environ. 14, 135–151.
Jackson, T.J., 1993. III. Measuring surface soil moisture using passive microwave remote sensing. Hydrol. Process. 7, 139–152.
Jackson, T.J., Chen, D., Cosh, M., Li, F., Anderson, M., Walthall, C., Doriaswamy, P., Hunt, E.R., 2004. Vegetation water content mapping using Landsat data derived normalized difference water index for corn and soybeans. Remote Sens. Environ. 92, 475–482.
Jackson, T.J., Le Vine, D.M., Hsu, A.Y., Oldak, A., Starks, P.J., Swift, C.T., Isham, J.D., Haken, M., 1999. Soil moisture mapping at regional scales using microwave radiometry: The southern great plains hydrology experiment. *IEEE Trans. Geosci. Remote Sens.*, 37, 2136–2151.
Jones, L.A., Kimball, J.S., Podest, E., McDonald, K.C., Chan, S.K., Njoku, E.G., 2009. A method for deriving land surface moisture, vegetation optical depth, and open water fraction from AMSR-E. In: Proceedings of the 2009 IEEE International Geoscience and Remote Sensing Symposium, IGARSS 2009 (pp. III–916–III–919): IEEE.
Jones, M.O., Jones, L.A., Kimball, J.S., McDonald, K.C., 2011. Satellite passive microwave remote sensing for monitoring global land surface phenology. Remote Sens. Environ. 115, 1102–1114.
Joseph, A.T., van der Velde, R., O'Neill, P.E., Lang, R.H., Gish, T., 2008. Soil moisture retrieval during a corn growth cycle using L-band (1.6 GHz) radar observations. IEEE Trans. Geosci. Remote Sens. 46, 2365–2374.
Joseph, A., van der Velde, R., O'neill, P., Lang, R., Gish, T., 2010. Effects of corn on C-and L-band radar backscatter: A correction method for soil moisture retrieval. Remote Sens. Environ. 114, 2417–2430.
Justice, C., Townshend, J., Choudhury, B., 1989. Comparison of AVHRR and SMMR data for monitoring vegetation phenology on a continental scale. Int. J. Remote Sens. 10, 1607–1632.
Karthikeyan L., Pan, M., Konings, A., Piles, M., Nagesh Kumar, D., Wood, E.F., 2017. Global scale simultaneous retrieval of vegetation optical depth, surface roughness, and soil moisture using AMSR-E observations. (In preparation).
Kelly, R., Davie, T., Atkinson, P.M., 2003. Explaining temporal and spatial variation in soil moisture in a bare field using SAR imagery. Int. J. Remote Sens. 24, 3059–3074.
Kerr, Y.H., Al-Yaari, A., Rodriguez-Fernandez, N., Parrens, M., Molero, B., Leroux, D., Bircher, S., Mahmoodi, A., Mialon, A., Richaume, P., 2016. Overview of SMOS performance in terms of global soil moisture monitoring after six years in operation. Remote Sens. Environ. 180, 40–63.
Kerr, Y.H., Njoku, E.G., 1990. A semiempirical model for interpreting microwave emission from semiarid land surfaces as seen from space. IEEE Trans. Geosci. Remote Sens. 28, 384–393.
Kerr, Y.H., Waldteufel, P., Richaume, P., Wigneron, J.P., Ferrazzoli, P., Mahmoodi, A., Al Bitar, A, Cabot, F, Gruhier, C., Juglea, S.E., 2012. The SMOS soil moisture retrieval algorithm. IEEE Trans. Geosci. Remote Sens. 50, 1384–1403.
Kirchhoff, G., 1860. I. On the relation between the radiating and absorbing powers of different bodies for light and heat. Lond. Edinburgh Dublin Philosoph. Mag. J. Sci. 20, 1–21.
Kirdiashev, K., Chukhlantsev, A., Shutko, A., 1979. Microwave radiation of the earth's surface in the presence of vegetation cover. Radiotekhnika I Elektronika, 24, 256–264.
Konings, A.G., Piles, M., Das, N., Entekhabi, D., 2017. L-band vegetation optical depth and effective scattering albedo estimation from SMAP. Remote Sens. Environ. 198, 460–470.
Konings, A.G., Piles, M., Rötzer, K., McColl, K.A., Chan, S.K., Entekhabi, D., 2016. Vegetation optical depth and scattering albedo retrieval using time series of dual-polarized L-band radiometer observations. Remote Sens. Environ. 172, 178–189.
Koster, R.D., Dirmeyer, P.A., Guo, Z., Bonan, G., Chan, E., Cox, P., Gordon, C., Kanae, S., Kowalczyk, E., Lawrence, D., 2004. Regions of strong coupling between soil moisture and precipitation. Science 305, 1138–1140.
Koster, R.D., Suarez, M.J., 2003. Impact of land surface initialization on seasonal precipitation and temperature prediction. J. Hydrometeorol. 4, 408–423.
Kurum, M., 2013. Quantifying scattering albedo in microwave emission of vegetated terrain. Remote Sens. Environ. 129, 66–74.
Kurum, M., Lang, R.H., O'Neill, P.E., Joseph, A.T., Jackson, T.J., Cosh, M.H., 2011. A first-order radiative transfer model for microwave radiometry of forest canopies at L-band. IEEE Trans. Geosci. Remote Sens. 49, 3167–3179.
Lakshmi, V., 2013. Remote sensing of soil moisture. ISRN Soil Sci. 2013.

Landau, L.D., Lifshitz, E., 1960. Course of theoretical physics. Electrodynamics of Continuous Media, Oxford, 8.
Lawrence, H., Wigneron, J.-P., Demontoux, F., Mialon, A., Kerr, Y.H., 2013. Evaluating the Semiempirical H–Q Model Used to Calculate the L-Band Emissivity of a Rough Bare Soil. IEEE Trans. Geosci. Remote Sens. 51, 4075–4084.
Le Hégarat-Mascle, S., Zribi, M., Alem, F., Weisse, A., Loumagne, C., 2002. Soil moisture estimation from ERS/SAR data: Toward an operational methodology. IEEE Trans. Geosci. Remote Sens. 40, 2647–2658.
Lievens, H., Vernieuwe, H., Alvarez-Mozos, J., De Baets, B., Verhoest, N.E., 2009. Error in radar-derived soil moisture due to roughness parameterization: An analysis based on synthetical surface profiles. Sensors 9, 1067–1093.
Liu, C., Shi, J., 2016. Estimation of vegetation parameters of water cloud model for global soil moisture retrieval using time-series L-Band Aquarius observations. IEEE J. Sel. Top. Appl. Earth Observ. Remote Sens. 9, 5621–5633.
Liu, P.-W., Judge, J., DeRoo, R.D., England, A.W., Bongiovanni, T., Luke, A., 2016. Dominant backscattering mechanisms at L-band during dynamic soil moisture conditions for sandy soils. Remote Sens. Environ. 178, 104–112.
Liu, S.-F., Liou, Y.-A., Wang, W.-J., Wigneron, J.-P., Lee, J.-B., 2002. Retrieval of crop biomass and soil moisture from measured 1.4 and 10.65 GHz brightness temperatures. IEEE Trans. Geosci. Remote Sens. 40, 1260–1268.
Liu, Y.Y., de Jeu, R.A., McCabe, M.F., Evans, J.P., van Dijk, A.I., 2011. Global long-term passive microwave satellite-based retrievals of vegetation optical depth. Geophys. Res. Lett. 38.
MacDonald, H.C., Waite, W.P., 1971. Soil moisture detection with imaging radars. Water Resourc. Res. 7, 100–110.
Manzoni, S., Vico, G., Palmroth, S., Porporato, A., Katul, G., 2013. Optimization of stomatal conductance for maximum carbon gain under dynamic soil moisture. Adv. Water Resourc. 62, 90–105.
McNairn, H., Jackson, T.J., Wiseman, G., Belair, S., Berg, A., Bullock, P., Colliander, A., Cosh, M.H., Kim, S.-B., Magagi, R., 2015. The soil moisture active passive validation experiment 2012 (SMAPVEX12): Prelaunch calibration and validation of the SMAP soil moisture algorithms. IEEE Trans. Geosci. Remote Sens. 53, 2784–2801.
Mironov, V.L., Kosolapova, L.G., Fomin, S.V., 2009. Physically and mineralogically based spectroscopic dielectric model for moist soils. IEEE Trans. Geosci. Remote Sens. 47, 2059–2070.
Mladenova, I., Jackson, T., Njoku, E., Bindlish, R., Chan, S., Cosh, M., Holmes, T., De Jeu, R., Jones, L., Kimball, J., 2014. Remote monitoring of soil moisture using passive microwave-based techniques—Theoretical basis and overview of selected algorithms for AMSR-E. Remote Sens. Environ. 144, 197–213.
Mo, T., Choudhury, B., Schmugge, T., Wang, J., Jackson, T., 1982. A model for microwave emission from vegetation-covered fields. J. Geophys. Res. Oceans 87, 11229–11237.
Mo, T., Schmugge, T.J., 1987. A parameterization of the effect of surface roughness on microwave emission. IEEE Trans. Geosci. Remote Sens. 481–486.
Mo, T., Schmugge, T.J., Jackson, T.J., 1984. Calculations of radar backscattering coefficient of vegetation-covered soils. Remote Sens. Environ. 15, 119–133.
Mohammed, P.N., Aksoy, M., Piepmeier, J.R., Johnson, J.T., Bringer, A., 2016. SMAP L-band microwave radiometer: rfi mitigation prelaunch analysis and first year on-orbit observations. IEEE Trans. Geosci. Remote Sens. 54, 6035–6047.
Montpetit, B., Royer, A., Wigneron, J.-P., Chanzy, A., Mialon, A., 2015. Evaluation of multi-frequency bare soil microwave reflectivity models. Remote Sens. Environ. 162, 186–195.
Moran, M.S., Hymer, D.C., Qi, J., Sano, E.E., 2000. Soil moisture evaluation using multi-temporal synthetic aperture radar (SAR) in semiarid rangeland. Agri. Forest Meteorol. 105, 69–80.
Moran, M.S., Peters-Lidard, C.D., Watts, J.M., McElroy, S., 2004. Estimating soil moisture at the watershed scale with satellite-based radar and land surface models. Can. J. Remote Sens. 30, 805–826.
Naeimi, V., Bartalis, Z., Wagner, W., 2009a. ASCAT soil moisture: An assessment of the data quality and consistency with the ERS scatterometer heritage. J. Hydrometeorol. 10, 555–563.
Naeimi, V., Scipal, K., Bartalis, Z., Hasenauer, S., Wagner, W., 2009b. An improved soil moisture retrieval algorithm for ERS and METOP scatterometer observations. IEEE Trans. Geosci. Remote Sens. 47, 1999–2013.
Narvekar, P.S., Entekhabi, D., Kim, S.-B., Njoku, E.G., 2015. Soil moisture retrieval using L-band radar observations. IEEE Trans. Geosci. Remote Sens. 53, 3492–3506.
Newton, R.W., 1977. Microwave remote sensing and its application to soil moisture detection. E78-10069, NASA–CR–151612, RSC–81. Texas A&M Univ.; Remote Sensing Center.; College Station, TX, United States.
Njoku, E.G., Chan, S.K., 2006. Vegetation and surface roughness effects on AMSR-E land observations. Remote Sens. Environ. 100, 190–199.
Njoku, E.G., Jackson, T.J., Lakshmi, V., Chan, T.K., Nghiem, S.V., 2003. Soil moisture retrieval from AMSR-E. IEEE Trans. Geosci. Remote Sens. 41, 215–229.
Njoku, E.G., Kong, J.A., 1977. Theory for passive microwave remote sensing of near–surface soil moisture. J. Geophys. Res. 82, 3108–3118.
Njoku, E.G., Li, L., 1999. Retrieval of land surface parameters using passive microwave measurements at 6-18 GHz. IEEE Trans. Geosci. Remote Sens. 37, 79–93.
Ogilvy, J.A., Ogilvy, J., 1991. Theory of Wave Scattering from Random Rough Surfaces. Hilger Bristol et al.
Oh, Y., 2004. Quantitative retrieval of soil moisture content and surface roughness from multipolarized radar observations of bare soil surfaces. IEEE Trans. Geosci. Remote Sens. 42, 596–601.
Oh, Y., Kay, Y.C., 1998. Condition for precise measurement of soil surface roughness. IEEE Trans. Geosci. Remote Sens. 36, 691–695.
Oh, Y., Sarabandi, K., Ulaby, F.T., 1992. An empirical model and an inversion technique for radar scattering from bare soil surfaces. IEEE Trans. Geosci. Remote Sens. 30, 370–381.
Oh, Y., Sarabandi, K., Ulaby, F.T., 1994. An inversion algorithm for retrieving soil moisture and surface roughness from polarimetric radar observation. In: Proceedings of the International Geoscience and Remote Sensing Symposium, 1994. IGARSS'94. Surface and Atmospheric Remote Sensing: Technologies, Data Analysis and Interpretation., pp. 1582–1584. IEEE.
Oh, Y., Sarabandi, K., Ulaby, F.T., 2002. Semi-empirical model of the ensemble-averaged differential Mueller matrix for microwave backscattering from bare soil surfaces. IEEE Trans. Geosci. Remote Sens. 40, 1348–1355.
Oliva, R., Daganzo, E., Richaume, P., Kerr, Y., Cabot, F., Soldo, Y., Anterrieu, E., Reul, N., Gutierrez, A., Barbosa, J., 2016. Status of Radio Frequency Interference (RFI) in the 1400–1427 MHz passive band based on six years of SMOS mission. Remote Sens. Environ. 180, 64–75.
Ouellette, J.D., Johnson, J.T., Balenzano, A., Mattia, F., Satalino, G., Kim, S.-B., Dunbar, R.S., Colliander, A., Cosh, M.H., Caldwell, T.G., 2017. A time-series approach to estimating soil moisture from vegetated surfaces using L-band radar backscatter. IEEE Trans. Geosci. Remote Sens. 55, 3186–3193.
Owe, M., de Jeu, R., Holmes, T., 2008. Multisensor historical climatology of satellite-derived global land surface moisture. J. Geophys. Res. Earth Surf. 113.
Owe, M., de Jeu, R., Walker, J., 2001. A methodology for surface soil moisture and vegetation optical depth retrieval using the microwave polarization difference index. IEEE Trans. Geosci. Remote Sens. 39, 1643–1654.
Paloscia, S., Pettinato, S., Santi, E., Notarnicola, C., Pasolli, L., Reppucci, A., 2013. Soil moisture mapping using Sentinel-1 images: Algorithm and preliminary validation. Remote Sens. Environ. 134, 234–248.
Paloscia, S., Santi, E., Pettinato, S., Mladenova, I., Jackson, T., Bindlish, R., Cosh, M., 2015. A comparison between two algorithms for the retrieval of soil moisture using AMSR-E data. Frontiers Earth Sci. 3, 16.
Pan, M., Sahoo, A.K., Wood, E.F., 2014. Improving soil moisture retrievals from a physically-based radiative transfer model. Remote Sens. Environ. 140, 130–140.
Panciera, R., Tanase, M.A., Lowell, K., Walker, J.P., 2014a. Evaluation of IEM, Dubois, and Oh radar backscatter models using airborne L-band SAR. IEEE Trans. Geosci. Remote Sens. 52, 4966–4979.
Panciera, R., Walker, J.P., Jackson, T.J., Gray, D.A., Tanase, M.A., Ryu, D., Monerris, A., Yardley, H., Rudiger, C., Wu, X., 2014b. The soil moisture active passive experiments (SMAPEx): Toward soil moisture retrieval from the SMAP mission. IEEE Trans. Geosci. Remote Sens. 52, 490–507.
Panciera, R., Walker, J.P., Merlin, O., 2009. Improved understanding of soil surface roughness parameterization for L-band passive microwave soil moisture retrieval. IEEE Geosci. Remote Sens. Lett. 6, 625–629.
Parrens, M., Wigneron, J.-P., Richaume, P., Al Bitar, A., Mialon, A., Fernandez–Moran, R., Al-Yaari, A., O'Neill, P., Kerr, Y., 2017. Considering combined or separated roughness and vegetation effects in soil moisture retrievals. Int. J. Appl. Earth Observ. Geoinform. 55, 73–86.
Parrens, M., Wigneron, J.-P., Richaume, P., Mialon, A., Al Bitar, A., Fernandez–Moran, R., Al-Yaari, A., Kerr, Y.H., 2016. Global-scale surface roughness effects at L-band as estimated from SMOS observations. Remote Sens. Environ. 181, 122–136.
Peischl, S., Walker, J.P., Ryu, D., Kerr, Y.H., Panciera, R., Rudiger, C., 2012. Wheat canopy structure and surface roughness effects on multiangle observations at L-band. IEEE Trans. Geosci. Remote Sens. 50, 1498–1506.
Pellarin, T., Calvet, J.-C., Wigneron, J.-P., 2003a. Surface soil moisture retrieval from L-band radiometry: a global regression study. IEEE Trans. Geosci. Remote Sens. 41, 2037–2051.
Pellarin, T., Wigneron, J.-P., Calvet, J.-C., Berger, M., Douville, H., Ferrazzoli, P., Kerr, Y.H., Lopez-Baeza, E., Pulliainen, J., Simmonds, L.P., 2003b. Two-year global simulation of L-band brightness temperatures over land. IEEE Trans. Geosci. Remote Sens. 41, 2135–2139.
Peng, B., Zhao, T., Shi, J., Lu, H., Mialon, A., Kerr, Y.H., Liang, X., Guan, K., 2017. Reappraisal of the roughness effect parameterization schemes for L-band radiometry over bare soil. Remote Sens. Environ. 199, 63–77.
Poe, G., Edgerton, A., 1971. Determination of soil moisture content with airborne microwave radiometry. 4006 R–1, DOC contract 1–35378. El Monte, California: Aerojet-General Corp., Microwave Division.
Poe, G., Stogryn, A., Edgerton, A., 1971. Determination of soil moisture content using microwave radiometry. 1684FR–1 DOC contract 0–35239. El Monte, California: Aerojet-General Corp., Microwave Division.
Prevot, L., Dechambre, M., Taconet, O., Vidal-Madjar, D., Normand, M., Gallej, S., 1993. Estimating the characteristics of vegetation canopies with airborne radar measurements. Int. J. Remote Sens. 14, 2803–2818.
Prigent, C., Rossow, W.B., Matthews, E., 1997. Microwave land surface emissivities estimated from SSM/I observations. J. Geophys. Res. Atmosph. 102, 21867–21890.
Pulliainen, J., Hallikainen, M., 2001. Retrieval of regional snow water equivalent from space-borne passive microwave observations. Remote Sens. Environ. 75, 76–85.
Rahman, M., Moran, M., Thoma, D., Bryant, R., Collins, C.H., Jackson, T., Orr, B.J., Tischler, M., 2008. Mapping surface roughness and soil moisture using multi-angle radar imagery without ancillary data. Remote Sens. Environ. 112, 391–402.
Rahman, M., Moran, M., Thoma, D., Bryant, R., Sano, E., Holifield Collins, C., Skirvin, S., Kershner, C., Orr, B.J., 2007. A derivation of roughness correlation length for parameterizing radar backscatter models. Int. J. Remote Sens. 28, 3995–4012.

Raju, S., Chanzy, A., Wigneron, J.-P., Calvet, J.-C., Kerr, Y., Laguerre, L., 1995. Soil moisture and temperature profile effects on microwave emission at low frequencies. Remote Sens. Environ. 54, 85–97.

Rao, K., Raju, S., Wang, J.R., 1993. Estimation of soil moisture and surface roughness parameters from backscattering coefficient. IEEE Trans. Geosci. Remote Sens. 31, 1094–1099.

Rice, S.O., 1951. Reflection of electromagnetic waves from slightly rough surfaces. Commun. Pure Appl. Math. 4, 351–378.

Rodríguez-Fernández, N.J., Aires, F., Richaume, P., Kerr, Y.H., Prigent, C., Kolassa, J., Cabot, F., Jiménez, C., Mahmoodi, A., Drusch, M., 2015. Soil moisture retrieval using neural networks: application to SMOS. IEEE Trans. Geosci. Remote Sens. 53, 5991–6007.

Roth, K., Schulin, R., Flühler, H., Attinger, W., 1990. Calibration of time domain reflectometry for water content measurement using a composite dielectric approach. Water Resourc. Res. 26, 2267–2273.

Saleh, K., Wigneron, J.-P., De Rosnay, P., Calvet, J.-C., Escorihuela, M.J., Kerr, Y., Waldteufel, P., 2006a. Impact of rain interception by vegetation and mulch on the L-band emission of natural grass. Remote Sens. Environ. 101, 127–139.

Saleh, K., Wigneron, J.-P., de Rosnay, P., Calvet, J.-C., Kerr, Y., 2006b. Semi-empirical regressions at L-band applied to surface soil moisture retrievals over grass. Remote Sens. Environ. 101, 415–426.

Saleh, K., Wigneron, J.-P., Waldteufel, P., De Rosnay, P., Schwank, M., Calvet, J.-C., Kerr, Y., 2007. Estimates of surface soil moisture under grass covers using L-band radiometry. Remote Sens. Environ. 109, 42–53.

Saleh, K., Wigneron, J., Calvet, J., Lopez-Baeza, E., Ferrazzoli, P., Berger, M., Wursteisen, P., Simmonds, L., Miller, J., 2004. The EuroSTARRS airborne campaign in support of the SMOS mission: First results over land surfaces. Int. J. Remote Sens. 25, 177–194.

Santi, E., Paloscia, S., Pettinato, S., Fontanelli, G., 2016. Application of artificial neural networks for the soil moisture retrieval from active and passive microwave spaceborne sensors. Int. J. Appl. Earth Observ. Geoinform. 48, 61–73.

Santi, E., Pettinato, S., Paloscia, S., Pampaloni, P., Macelloni, G., Brogioni, M., 2012. An algorithm for generating soil moisture and snow depth maps from microwave spaceborne radiometers: HydroAlgo. Hydrol. Earth Syst. Sci. 16, 3659–3676.

Satalino, G., Mattia, F., Davidson, M.W., Le Toan, T., Pasquariello, G., Borgeaud, M., 2002. On current limits of soil moisture retrieval from ERS-SAR data. IEEE Trans. Geosci. Remote Sens. 40, 2438–2447.

Schanda, E., 1987. On the contribution of volume scattering to the microwave backscattered signal from wet snow and wet soil. Int. J. Remote Sens. 8, 1489–1500.

Schanda, E., Hofer, R., Wyssen, D., Musy, A., Meylan, D., Morzier, C., Good, W., 1978. Soil moisture determination and snow classification with microwave radiometry. In: Proceedings of the 12th International Symposium on Remote Sensing of Environment, pp. 1779–1789.

Schmugge, T., 1978. Remote sensing of surface soil moisture. J. Appl. Meteorol. 17, 1549–1557.

Schmugge, T., 1987. Remote sensing applications in hydrology. Rev. Geophys. 25, 148–152.

Schmugge, T., Gloersen, P., Wilheit, T., Geiger, F., 1974. Remote sensing of soil moisture with microwave radiometers. J. Geophys. Res. 79, 317–323.

Schmugge, T., Jackson, T., 1994. Mapping surface soil moisture with microwave radiometers. Meteorol. Atmosph. Phys. 54, 213–223.

Schmugge, T., Jackson, T., McKim, H., 1980. Survey of methods for soil moisture determination. Water Resourc. Res. 16, 961–979.

Schmugge, T., Meneely, J., Rango, A., Neff, R., 1977. Satellite microwave observations of soil moisture variations. JAWRA J. Am. Water Resourc. Assoc. 13, 265–282.

Schmugge, T., Wang, J., Asrar, G., 1988. Results from the push broom microwave radiometer flights over the Konza Prairie in 1985. IEEE Trans. Geosci. Remote Sens. 26, 590–596.

Seneviratne, S.I., Corti, T., Davin, E.L., Hirschi, M., Jaeger, E.B., Lehner, I., Orlowsky, B., Teuling, A.J., 2010. Investigating soil moisture–climate interactions in a changing climate: A review. Earth-Sci. Rev. 99, 125–161.

Shi, J., Chen, K.-S., Li, Q., Jackson, T.J., O'Neill, P.E., Tsang, L., 2002. A parameterized surface reflectivity model and estimation of bare-surface soil moisture with L-band radiometer. IEEE Trans. Geosci. Remote Sens. 40, 2674–2686.

Shi, J., Wang, J., Hsu, A.Y., O'Neill, P.E., Engman, E.T., 1997. Estimation of bare surface soil moisture and surface roughness parameter using L-band SAR image data. IEEE Trans. Geosci. Remote Sens. 35, 1254–1266.

Shoshany, M., Svoray, T., Curran, P., Foody, G.M., Perevolotsky, A., 2000. The relationship between ERS-2 SAR backscatter and soil moisture: generalization from a humid to semi-arid transect. Int. J. Remote Sens. 21, 2337–2343.

Stogryn, A., 1967. Electromagnetic scattering from rough, finitely conducting surfaces. Radio Sci. 2, 415–428.

Stogryn, A., 1970. The brightness temperature of a vertically structured medium. Radio Sci. 5, 1397–1406.

Teng, W., Wang, J., Doraiswamy, P., 1993. Relationship between satellite microwave radiometric data, antecedent precipitation index, and regional soil moisture. Int. J. Remote Sens. 14, 2483–2500.

Theis, S.W., Blanchard, B.J., Newton, R.W., 1984. Utilization of vegetation indices to improve microwave soil moisture estimates over agricultural lands. IEEE Trans. Geosci. Remote Sens. 490–496.

Thoma, D., Moran, M., Bryant, R., Collins, C.H., Rahman, M., Skirvin, S., 2004. Comparison of two methods for extracting surface soil moisture from C-band radar imagery. In: Proceedings of the 2004 IEEE International Geoscience and Remote Sensing Symposium, pp. 827–830. IEEE.

Thoma, D., Moran, M., Bryant, R., Rahman, M., Holifield-Collins, C., Skirvin, S., Sano, E., Slocum, K., 2006. Comparison of four models to determine surface soil moisture from C-band radar imagery in a sparsely vegetated semiarid landscape. Water Resourc. Res. 42.

Tomer, S.K., Al Bitar, A., Sekhar, M., Zribi, M., Bandyopadhyay, S., Sreelash, K., Sharma, A., Corgne, S., Kerr, Y., 2015. Retrieval and multi-scale validation of soil moisture from multi-temporal SAR data in a semi-arid tropical region. Remote Sens. 7, 8128–8153.

Topp, G.C., Davis, J., Annan, A.P., 1980. Electromagnetic determination of soil water content: Measurements in coaxial transmission lines. Water Resourc. research 16, 574–582.

Tsang, L., Kong, J.A., Shin, R.T., 1985. Theory of Microwave Remote Sensing. Wiley, New York.

Ulaby, F., 1974. Radar measurement of soil moisture content. IEEE Trans. Antennas and Prop. 22, 257–265.

Ulaby, F., Cihlar, J., Moore, R., 1974. Active microwave measurement of soil water content. Remote Sens. Environ. 3, 185–203.

Ulaby, F., Moore, R., Fung, A., 1982. Microwave remote sensing: Active and Passive, 2-Radar Remote Sensing and Surface Scattering and Emission Theory.

Ulaby, F., Moore, R., Fung, A., 1986. Microwave Remote Sensing: Active and Passive, 3-From Theory to Applications.

Ulaby, F.T., Batlivala, P.P., 1976. Optimum radar parameters for mapping soil moisture. IEEE Trans. Geosci. Electron. 14, 81–93.

Ulaby, F.T., Batlivala, P.P., Dobson, M.C., 1978. Microwave backscatter dependence on surface roughness, soil moisture, and soil texture: Part I-bare soil. IEEE Trans. Geosci. Electron. 16, 286–295.

Ulaby, F.T., Dubois, P.C., Van Zyl, J., 1996. Radar mapping of surface soil moisture. J. Hydrol. 184, 57–84.

Ulaby, F.T., Razani, M., Dobson, M.C., 1983. Effects of vegetation cover on the microwave radiometric sensitivity to soil moisture. IEEE Trans. Geosci. Remote Sens. 51–61.

Ulaby, F.T., Sarabandi, K., Mcdonald, K., Whitt, M., Dobson, M.C., 1990. Michigan microwave canopy scattering model. Int. J. Remote Sens. 11, 1223–1253.

Van de Griend, A.A., Wigneron, J.-P., 2004. On the measurement of microwave vegetation properties: Some guidelines for a protocol. IEEE Trans. Geosci. Remote Sens. 42, 2277–2289.

Verhoest, N.E., Lievens, H., Wagner, W., Álvarez-Mozos, J., Moran, M.S., Mattia, F., 2008. On the soil roughness parameterization problem in soil moisture retrieval of bare surfaces from synthetic aperture radar. Sensors 8, 4213–4248.

Vittucci, C., Ferrazzoli, P., Kerr, Y., Richaume, P., Guerriero, L., Rahmoune, R., Laurin, G.V., 2016. SMOS retrieval over forests: Exploitation of optical depth and tests of soil moisture estimates. Remote Sens. Environ. 180, 115–127.

Voronovich, A., 1985. Small-slope approximation in wave scattering by rough surfaces. Sov. Phys. JETP 62, 65–70.

Vreugdenhil, M., Dorigo, W.A., Wagner, W., de Jeu, R.A., Hahn, S., van Marle, M.J., 2016. Analyzing the Vegetation Parameterization in the TU-Wien ASCAT Soil Moisture Retrieval. IEEE Trans. Geosci. Remote Sens. 54, 3513–3531.

Wagner, W., 1998. Soil moisture retrieval from ERS scatterometer data. Citeseer.

Wagner, W., Blöschl, G., Pampaloni, P., Calvet, J.-C., Bizzarri, B., Wigneron, J.-P., Kerr, Y., 2007. Operational readiness of microwave remote sensing of soil moisture for hydrologic applications. Hydrol. Rese. 38, 1–20.

Wagner, W., Lemoine, G., Borgeaud, M., Rott, H., 1999a. A study of vegetation cover effects on ERS scatterometer data. IEEE Trans. Geosci. Remote Sens. 37, 938–948.

Wagner, W., Lemoine, G., Rott, H., 1999b. A method for estimating soil moisture from ERS scatterometer and soil data. Remote Sens. Environ. 70, 191–207.

Wagner, W., Scipal, K., 2000. Large-scale soil moisture mapping in western Africa using the ERS scatterometer. IEEE Trans. Geosci. Remote Sens. 38, 1777–1782.

Wagner, W., Scipal, K., Pathe, C., Gerten, D., Lucht, W., Rudolf, B., 2003. Evaluation of the agreement between the first global remotely sensed soil moisture data with model and precipitation data. J. Geophys. Res. Atmosph. 108.

Walker, J.P., Houser, P.R., Willgoose, G.R., 2004. Active microwave remote sensing for soil moisture measurement: a field evaluation using ERS-2. Hydrol. Process. 18, 1975–1997.

Wanders, N., Bierkens, M.F., de Jong, S.M., de Roo, A., Karssenberg, D., 2014a. The benefits of using remotely sensed soil moisture in parameter identification of large-scale hydrological models. Water Resourc. Res. 50, 6874–6891.

Wanders, N., Karssenberg, D., Roo, A.d., De Jong,, S., Bierkens, M., 2014b. The suitability of remotely sensed soil moisture for improving operational flood forecasting. Hydrol. Earth Syst. Sci. 18, 2343–2357.

Wanders, N., Pan, M., Wood, E., 2015. Correction of real-time satellite precipitation with multi-sensor satellite observations of land surface variables. Remote Sens. Environ. 160, 206–221.

Wang, H., Méric, S., Allain, S., Pottier, E., 2015a. Multi-angular ground-based SAR system for soil surface roughness characterisation. Electron. Lett. 51, 1197–1199.

Wang, J., Choudhury, B., 1981. Remote sensing of soil moisture content, over bare field at 1.4 GHz frequency. J. Geophys. Res. Oceans 86, 5277–5282.

Wang, J., Shiue, J., Schmugge, T., Engman, E., 1990. The L-band PBMR measurements of surface soil moisture in FIFE. IEEE Trans. Geosci. Remote Sens. 28, 906–914.

Wang, J.R., Engmen, E.T., Shiue, J.C., Rusek, M., Steinmeier, C., 1986. The SIR-B observations of microwave backscatter dependence on soil moisture, surface roughness, and vegetation covers. IEEE Trans. Geosci. Remote Sens. 510–516.

Wang, J.R., McMurtrey, J.E., Engman, E.T., Jackson, T.J., Schmugge, T.J., Gould, W.I., Fuchs, J.E., Glazar, W.S., 1982. Radiometric measurements over bare and vegetated fields at 1.4-GHz and 5-GHz frequencies. Remote Sens. Environ. 12, 295–311.

Wang, J.R., Schmugge, T.J., 1980. An empirical model for the complex dielectric permittivity of soils as a function of water content. IEEE Trans. Geosci. Remote Sens. 288–295.
Wang, S., Wigneron, J.-P., Jiang, L.-M., Parrens, M., Yu, X.-Y., Al-Yaari, A., Ye, Q.-Y., Fernandez-Moran, R., Ji, W., Kerr, Y., 2015b. Global-scale evaluation of roughness effects on C-band AMSR-E observations. Remote Sens. 7, 5734–5757.
Wegmüller, U., Matzler, C., 1999. Rough bare soil reflectivity model. IEEE Trans. Geosci. Remote Sens. 37, 1391–1395.
Weimann, A., Von Schonermark, M., Schumann, A., Jorn, P., Gunther, R., 1998. Soil moisture estimation with ERS-1 SAR data in the East-German loess soil area. Int. J. Remote Sens. 19, 237–243.
Wigneron, J.-P., Calvet, J.-C., De Rosnay, P., Kerr, Y., Waldteufel, P., Saleh, K., Escorihuela, M.J., Kruszewski, A., 2004. Soil moisture retrievals from biangular L-band passive microwave observations. IEEE Geosci. Remote Sens. Lett. 1, 277–281.
Wigneron, J.-P., Calvet, J.-C., Pellarin, T., Van de Griend, A., Berger, M., Ferrazzoli, P., 2003. Retrieving near-surface soil moisture from microwave radiometric observations: current status and future plans. Remote Sens. Environ. 85, 489–506.
Wigneron, J.-P., Chanzy, A., Calvet, J.-C., Bruguier, N., 1995. A simple algorithm to retrieve soil moisture and vegetation biomass using passive microwave measurements over crop fields. Remote Sens. Environ. 51, 331–341.
Wigneron, J.-P., Chanzy, A., De Rosnay, P., Rudiger, C., Calvet, J.-C., 2008. Estimating the effective soil temperature at L-band as a function of soil properties. IEEE Trans. Geosci. Remote Sens. 46, 797–807.
Wigneron, J.-P., Kerr, Y., Waldteufel, P., Saleh, K., Escorihuela, M.-J., Richaume, P., Ferrazzoli, P., De Rosnay, P., Gurney, R., Calvet, J.-C., 2007. L-band microwave emission of the biosphere (L-MEB) model: Description and calibration against experimental data sets over crop fields. Remote Sens. Environ. 107, 639–655.
Wigneron, J.-P., Laguerre, L., Kerr, Y.H., 2001. A simple parameterization of the L-band microwave emission from rough agricultural soils. IEEE Trans. Geosci. Remote Sens. 39, 1697–1707.
Wigneron, J.-P., Waldteufel, P., Chanzy, A., Calvet, J.-C., Kerr, Y., 2000. Two-dimensional microwave interferometer retrieval capabilities over land surfaces (SMOS mission). Remote Sens. Environ. 73, 270–282.
Wilheit, T.T., 1978. Radiative transfer in a plane stratified dielectric. IEEE Trans. Geosci. Electron. 16, 138–143.
Wu, T.-D., Chen, K.-S., Shi, J., Fung, A.K., 2001. A transition model for the reflection coefficient in surface scattering. IEEE Trans. Geosci. Remote Sens. 39, 2040–2050.
Yuan, X., Ma, Z., Pan, M., Shi, C., 2015. Microwave remote sensing of short-term droughts during crop growing seasons. Geophys. Res. Lett. 42, 4394–4401.
Zhan, W., Pan, M., Wanders, N., Wood, E., 2015. Correction of real-time satellite precipitation with satellite soil moisture observations. Hydrol. Earth Syst. Sci. 19, 4275–4291.
Zribi, M., Dechambre, M., 2003. A new empirical model to retrieve soil moisture and roughness from C-band radar data. Remote Sens. Environ. 84, 42–52.
Zribi, M., Gorrab, A., Baghdadi, N., Lili-Chabaane, Z., Mougenot, B., 2014. Influence of radar frequency on the relationship between bare surface soil moisture vertical profile and radar backscatter. IEEE Geosci. Remote Sens. Lett. 11, 848–852.
Zribi, M., Le Hégarat-Mascle, S., Ottlé, C., Kammoun, B., Guerin, C., 2003. Surface soil moisture estimation from the synergistic use of the (multi-incidence and multi-resolution) active microwave ERS Wind Scatterometer and SAR data. Remote Sens. Environ. 86, 30–41.
Zribi, M., Taconet, O., Le Hégarat-Mascle, S., Vidal-Madjar, D., Emblanch, C., Loumagne, C., Normand, M., 1997. Backscattering behavior and simulation comparison over bare soils using SIR-C/X-SAR and ERASME 1994 data over Orgeval. Remote Sens. Environ. 59, 256–266.